

12-2011

Fault-Tree Model for Bridge Collapse Risk Analysis

Caitlyn Davis-mcdaniel

Clemson University, davismcdanie@live.marshall.edu

Follow this and additional works at: https://tigerprints.clemson.edu/all_theses

 Part of the [Civil Engineering Commons](#)

Recommended Citation

Davis-mcdaniel, Caitlyn, "Fault-Tree Model for Bridge Collapse Risk Analysis" (2011). *All Theses*. 1265.

https://tigerprints.clemson.edu/all_theses/1265

This Thesis is brought to you for free and open access by the Theses at TigerPrints. It has been accepted for inclusion in All Theses by an authorized administrator of TigerPrints. For more information, please contact kokeefe@clemson.edu.

FAULT-TREE MODEL FOR BRIDGE COLLAPSE RISK ANALYSIS

A Thesis
Presented to
the Graduate School of
Clemson University

In Partial Fulfillment
of the Requirements for the Degree
Masters of Science
Civil Engineering

by
Caitlyn E. Davis-McDaniel
December 2011

Accepted by:
Dr. Mashrur Chowdhury, Committee Chair
Dr. Weichiang Pang, Co-Committee Chair
Dr. Bradley Putman

ABSTRACT

Bridges are vital components of the United States surface transportation infrastructure and, moreover, support the growth of our nation's economy. However, over the past few decades the design capacity and service condition of many bridges in the U.S. has been challenged. Numerous incidents of bridge collapse call for an urgent need to develop a systematic method of assessing the failure risks and identifying the initiating events that can lead to a bridge collapse. This thesis presents a process of bridge failure risk analysis through fault-tree modeling and identification of specific countermeasures, to minimize failure risk, related to structural health monitoring (SHM).

The fault-tree analysis (FTA) process involves development of a visual fault-tree model, identification of minimal cut sets, assignment of basic event probabilities, and ranking of minimal cut sets according to probability of occurrence. The ranked minimal cut sets are used to identify SHM sensors that can reduce the causal factors associated with bridge failure.

The use of FTA as a risk assessment method for bridge collapse was found to be an improvement on current risk analysis methods, however, it is not a replacement. It is best used in combination with visual inspections and SHM sensors. The added benefits of FTA are its ability to identify initiating events to bridge failure through assessment of bridge components and their relationships to one another. It also has the advantage of being capable of assessing internal bridge components. These aspects make the qualitative analysis component of FTA a great tool for determining the initiating bridge

failure events. The deficiencies of FTA arise in quantitative analysis. There is often a lack of numerical data available on a basic event's contribution to bridge failure; however, expert opinion, sensitivity analysis, and probabilistic ranges can sometimes provide information accurate enough for use in countermeasure assessment and application. With validation data difficult to find, the accuracy of the quantitative results cannot be quantified with certainty; therefore, more reliable probabilistic data would make FTA a more successful bridge risk assessment tool.

ACKNOWLEDGMENTS

I would like to thank my primary advisors Mashrur Chowdhury and Weichiang Pang for their advice, guidance and support during my graduate career and Brad Putman for his comments and support as a member of my advisory committee. I would like to extend my thanks to David Wheeler, who served as an external reader of my thesis and provided editorial comments.

I am grateful for the information and resources provided to me by the SCDOT, particularly Lee Floyd, Eric Jones, Russel Aikens, Brandon Wilson, and the members of the District 3 bridge inspection team. I am also very grateful for the financial support from the National Science Foundation (NSF) and Clemson University. This research was supported by the National Science Foundation, under Grant No. NSF-1011478. The views and conclusions contained in this document are those of the writers and should not be interpreted as necessarily representing the official policies, either expressed or implied, of the National Science Foundation.

I would also like to acknowledge my fellow classmates and friends who provided a helping hand when I needed one. A special thanks to my family, especially my parents, who have always supported me in my educational endeavors. I could not have made it this far without all of you.

TABLE OF CONTENTS

	Page
TITLE PAGE	i
ABSTRACT	ii
ACKNOWLEDGMENTS	iv
LIST OF TABLES	vii
LIST OF FIGURES	x
CHAPTER	
1. INTRODUCTION	1
Bridge Failures in the United States	1
Bridge Failure Risk Analysis Methods	4
Research Objectives	6
2. LITERATURE REVIEW	7
Current Bridge Failure Risk Analysis Methods	7
Visual Inspection	7
Pontis Model	8
Ann Model	10
BRIDGIT Model	10
SHM Sensors	10
Post-Tensioned Concrete Box Girder Bridge Failure Risk Analysis	11
Lake View Drive Bridge Failure Case Study	16
Changes in Design and Construction Procedures	16
Fault-Tree Analysis as a Risk Assessment Tool	17
Summary and Discussion	20
3. RISK ASSESSMENT PROCESS AND METHODOLOGY	22
Fault-Tree Development	22
Minimal Cut Sets	23
Occurrence Probabilities	23
Countermeasures	25

Table of Contents (Continued)

	Page
Case Studies	27
Post-Tensioned Adjacent Concrete Box Girder Bridges	27
James B. Edwards Bridge in Charleston, SC	28
4. CASE STUDY: FAULT-TREE QUALITATIVE ANALYSIS FOR POST-TENSIONED ADJACENT CONCRETE BOX GIRDER BRIDGES	30
Fault-Tree Development	30
Superstructure Failures	33
Substructure Failures	35
Minimal Cut Sets	36
5. CASE STUDY: FAULT-TREE ANALYSIS FOR JAMES B. EDWARDS BRIDGE.....	38
Fault-Tree Development	38
Superstructure Failures	38
Substructure Failures	40
Minimal Cut Sets	40
Occurrence Probabilities.....	40
Countermeasures.....	47
6. CONCLUSIONS.....	49
APPENDIX A.....	52
APPENDIX B	54
APPENDIX C	58
APPENDIX D.....	74
REFERENCES	83

LIST OF TABLES

Table	Page
1-1 Top 15 Bridge Failures in the United States	1
1-2 Causes of Bridge Failures in the United States.....	2
2-1 National Bridge Inventory Condition Rating Guidelines	8
3-1 Bridge Failures Due to Concrete Deterioration and Corrosion	25
5-1 Annual Failure Probabilities Used for Fault-Tree Analysis	42
5-2 Top Five Minimal Cut Sets Based on Probability of Occurrence	45
5-3 Examples of SHM Sensors for Top Five Minimal Cut Sets.....	47
C-1 Data Used for Calculation of Probabilities	66
C-2 Minimal Cut Set Ranking Based on Probability of Occurrence	70
C-3 Examples of SHM Sensors for Applicable Minimal Cut Sets.....	71
D-1 Example Results: Substructure NBI Ratings and Corresponding Failure Probabilities	82

LIST OF FIGURES

Figure	Page
2-1 Concrete Box Girders (a) Adjacent (b) Segmental	13
2-2 Fault-Tree Gate Symbols and Descriptions	18
2-3 Fault-Tree Event Symbols and Descriptions	18
3-1 Sensor Detection Outcomes	26
3-2 Bridge Failure Due to Scour and Sensor Failure	27
3-3 James B. Edwards Bridge of Charleston, SC.....	28
3-4 SCDOT Inspection of James B. Edwards Bridge: (a) Improper Grouting of Ducts (b) Small Void Drain Holes (c) Cracks in Piers (d) Leaky Joints	29
4-1 Fault-Tree Model for Superstructure of Adjacent Box Girder Bridges	31
4-2 Fault-Tree Model for Substructure of Adjacent Box Girder Bridges	32
4-3 Fault-Tree Model for Tie Rod Access	34
4-4 Fault-Tree Model for Reinforcement Access	35
5-1 Fault-Tree Model for James B. Edwards Bridge Superstructure Failure.....	39
5-2 Fault-Tree Model for James B. Edwards Bridge Substructure Failure.....	41
5-3 NBI Rating Comparison of Segmental Bridges and All Bridge Types	44
5-4 Failure Probability and Reliability Index versus Age of the James B. Edwards Bridge.....	46
A-1 Isograph FaultTree+ Interface	53
B-1 Fault-Tree for Adjacent Box Girder Bridges	57
C-1 Roadway beneath James B. Edwards Bridge.....	59
C-2 James B. Edwards Bridge over Wando River.....	60

C-3	View Inside James B. Edwards Bridge.....	60
C-4	James B. Edwards Bridge: Grout Voids and Tendon Exposure in Ducts.....	61
C-5	James B. Edwards Bridge: Efflorescence from Leaky Joints	62
C-6	James B. Edwards Bridge: Leaky Joint with Exposed Rebar	63
C-7	James B. Edwards Bridge: Large Spall in Segment Roof near Joint.....	64
C-8	James B. Edwards Bridge Bearing.....	64
C-9	James B. Edwards Bridge Fault-Tree	67
C-10	NBI Superstructure Rating Error Comparison (a) Normalized Error (b) Mean (c) Variance	68
C-11	NBI Substructure Rating Error Comparison (a) Normalized Error (b) Mean (c) Variance	69
C-12	Example Application of Countermeasure to James B. Edwards Bridge	73
D-1	Median Estimate of NBI Ratings versus Bridge Age	76
D-2	Mean of Normalized Error versus Bridge Age	77
D-3	Variance of Normalized Error versus Bridge Age.....	78
D-4	Substructure Failure Probability versus Bridge Age	80

CHAPTER ONE

INTRODUCTION

Bridge Failure in the United States

There were 1,814 bridges (includes road, rail and pedestrian bridges) that failed between 1800 and 2009, according to a study conducted by Sharma and Mohan (2011). Road bridge failures accounted for 62% of those failures with 1,132 failures (Sharma and Mohan 2011). The top five bridge types to fail in order from the most to least failures are: beam/girder, truss, slab, stringer and arch bridges. When broken down to the type of bridge and material, the top five bridge failures occur in steel beam/girder, steel truss, concrete beam/girder, concrete slab and timber beam/girder bridges. A list of the top 15 bridge failures according to each category can be seen in Table 1-1.

Table 1-1. Top 15 Bridge Failures in the United States (Sharma and Mohan 2011)				
Bridge Type		Bridge Type and Material		
1	Beam/Girder	28.8%	1 Steel Beam/Girder	20.0%
2	Truss	24.5%	- Steel Truss	20.0%
3	Slab	4.8%	3 Concrete Beam/Girder	6.1%
4	Stringer	3.6%	4 Concrete Slab	4.7%
5	Arch	1.9%	5 Timber Beam/Girder	1.8%
6	Culvert	1.5%	- Timber Stringer	1.8%
7	Box Girder	1.3%	7 Steel Stringer	1.7%
8	Covered	1.2%	8 Timber Covered	1.2%
9	Span	1.0%	- Concrete Box Girder	1.2%
10	Cable	0.8%	10 Timber Truss	1.0%
11	Corrugated Pipe	0.3%	- Concrete Arch	1.0%
12	Box	0.2%	- Steel Culvert	1.0%
-	Bailey	0.2%	13 Steel Cable	0.8%
-	Tied Arch	0.2%	14 Steel Span	0.6%
15	Bascule	0.1%	15 Concrete Culvert	0.5%

Several different events cause these bridge failures. All the causes of bridge failure noted by Sharma and Mohan (2011) can be seen in Table 1-2. Hydraulic events are the leading causes of all bridge failures in the United States, accounting for over half of the failures. The leading hydraulic events were floods and scour, accounting for 38% and 11% of bridge failures, respectively (Sharma and Mohan 2011). Of these two failure modes, floods have been found to cause failure within the first two years of the bridge service life, where most scour failures take multiple years to occur (Smith 1976). Usually failure events take multiple years to occur, unless they are related to a catastrophic natural disaster or major design or construction error. The majority of these failure events may be prevented by identifying, quantifying and managing risks that occur over time.

Table 1-2. Causes of Bridge Failures in the United States (Sharma and Mohan 2011)	
Causes of Failure	% of Total Failures
Hydraulic	54.0
Collision	14.0
Overload	12.3
Deterioration	5.4
Fire	2.8
Design	1.3
Earthquake	1.1
Construction	1.0
Ice	1.0
Strom/Hurricane/Tsunami	0.9
Fatigued Steel	0.5
Soil	0.2
Miscellaneous	5.5

When bridge failures occur, they can have a significant effect on the economy and public well-being, which can be seen by the August 1, 2007 collapse of the I-35 Bridge over the Mississippi River in Minneapolis, MN. According to the National Transportation Safety Board Accident Report (2008), the collapse was the result of:

“...insufficient bridge design firm quality control procedures for designing bridges, and insufficient Federal and State procedures for reviewing and approving bridge design plans and calculations; lack of guidance for bridge owners with regard to the placement of construction loads on bridges during repair or maintenance activities; exclusion of gusset plates in bridge load rating guidance; lack of inspection guidance for conditions of gusset plate distortion; and inadequate use of technologies for accurately assessing the condition of gusset plates on deck truss bridges.”

The bridge was a 1,907-foot-long deck truss bridge consisting of eight lanes of which only four lanes were open to traffic the day of the collapse due to construction taking place on the bridge. At the time of failure, 111 vehicles were on the 456-foot portion of the main span that collapsed. The end result was 13 fatalities and 145 injuries (National Transportation Safety Board 2008). In addition to injuries and loss of life, the collapse had an effect on the transportation network. Since the I-35 Bridge no longer existed, the 140,000 vehicles that traveled the I-35 Bridge daily had to find a different route to cross the Mississippi River (Zhu et al. 2010). As a result, the number of vehicles on the remaining bridges crossing the Mississippi River increased an average of 21% and the

ridership of public transportation increased 6.6% (Zhu et al. 2010). These changes can have an effect on the condition of the remaining bridges and transportation.

The numerous bridge failures and their impacts portray a need for bridge management improvements; however, budget cut-backs have made the task of making needed repairs to bridges difficult (Pearson-Kirk 2008). This illustrates the need for a risk analysis tool to rank bridges according to their risk factor, which could help bridge managers decide where to focus their funds and efforts. With a proficient, systematic way to assess the risk of the bridges, the bridge management system could be more efficient and reduce the amount of bridge failures seen in the United States in the future.

Bridge Failure Analysis Methods

Current bridge risk analysis methods and tools developed are: visual bridge inspections, Structural Health Monitoring (SHM) sensors, computerized simulations, and computerized knowledge-based systems. The purpose of the visual inspections is to look for signs and symptoms of deterioration that could lead to failure. Structural health monitoring tools look for symptoms using sensors located on the bridge that can be connected to a computer network. Computerized models and simulations were created to predict failure based on historical data and trends. Two example computerized simulation models that have been developed are Pontis (Floyd 2010) and Artificial Neural Network (ANN) (Huang 2010). In addition to historical data and trends, computerized knowledge-based systems compile and input expert opinions and results from other methods (e.g. visual inspections). BRIDGIT is a two-component

computerized knowledge-based system (de Brito et al. 1997). More detail on how each of these risk analysis methods work will be provided in Chapter 2.

Each method discussed has some limitations or downfalls, many of which can be resolved using fault-tree analysis (FTA). Some of the limitations and FTA resolutions for the various methods are provided below:

- Visual inspections have difficulty assessing the condition of internal components. Often, invasive methods must be used to visually inspect internal components. FTA can assess internal components without any damage to bridge components.
- The computerized simulations and knowledge-based systems require a significant amount of technical data. FTA requires data to be input for probabilities, but it is not as technical or sizeable. In addition, if exact information is not known, an educated guess or probable range can be input for the probability.
- SHM, computerized simulation, and sometimes visual inspections do not identify the chain of events that lead to bridge failure. The fault-tree developed for FTA is developed using the chain of events; therefore, the events leading to failure can be identified through analysis.
- Many of the visual inspections, computerized simulations, and computerized knowledge-based systems discussed only assess the condition of individual components instead of individual components and the whole bridge system. FTA assesses the condition of individual components and identifies the relationships between the different components to assess the failure risk of the whole bridge system.

- With exception to some computerized simulations, all the methods mentioned are not known to utilize or produce a visual model of the bridge system. FTA produces a fault-tree model which visually shows the individual bridge components with the chain of events leading to their failure and ultimately bridge failure, as well as, the relationships between the bridge components.

Research Objectives

The objective of this research is to develop a bridge risk assessment process that can predict failure and its key initiators prior to the occurrence of failure symptoms, such as cracks, large deflections and corrosion. Due to the ability of fault-tree analysis (FTA) to qualitatively and quantitatively assess bridge failure, it is utilized to develop the risk assessment process for this research. An advantage of FTA qualitative assessment is its ability to visually model events leading to failure and their relationships, which can be used to define the most likely events to cause failure. The advantage of quantitative assessment is its ability to use a variety of input data to define expected occurrence probabilities of initiating events, which allows the assessment to take place prior to the construction of a bridge, if desired. The FTA process developed is used to identify the risk of bridge collapse, the events leading to collapse, and countermeasures to initiating events. Development of a process that is easily implementable by infrastructure managers can help them to make informed decisions about their infrastructure plans and budget allocations.

CHAPTER TWO

LITERATURE REVIEW

Current Bridge Failure Risk Analysis Methods

There are various types of bridge risk analysis methods that have been developed over the years. Some of the simplistic methods have been used for centuries, while others methods that utilize new technology have only been introduced in the last couple decades. This section will take a look at bridge risk analysis methods that are related to field inspections, computer simulations and on-site sensors. The particular methods to be discussed are: visual inspection, Pontis model, ANN model, BRIDGIT model and SHM sensors.

Visual Inspection

Visual bridge inspections are typically performed every two years, unless a bridge requires more frequent inspections due to safety concerns. During inspections, the bridge components are assigned a rating condition based on the National Bridge Inventory (NBI) guidelines (FHWA 1995), which are similar to those found in Table 2-1. The NBI rating system is used across the U.S. to standardize the condition ratings of bridges so the nation's bridge infrastructure can be assessed. The problem with these guidelines is that they assess symptoms, which are not always present (Naito et al. 2010b). Some of the conditions that are difficult or impossible to assess visually are:

- Corrosion of reinforcement encased in concrete (Naito et al. 2010a; Naito et al. 2010b; Russell 2009)

- Presence and deterioration of grout in shear keys and ducts (Naito et al. 2010b)
- Loss of post-tensioning in tendons (Naito et al. 2010b)
- Deterioration of epoxy in joints
- Insufficient concrete cover

Table 2-1. National Bridge Inventory Condition Rating Guidelines (FHWA 1995)

Rating	Description for Deck, Superstructure and Substructure
9	<u>Excellent</u>
8	<u>Very good</u> : no problems
7	<u>Good</u> : minor problems
6	<u>Satisfactory</u> : some minor deterioration of structural elements
5	<u>Fair</u> : primary structural elements are sound but may have minor section loss, cracking, spalling or scour
4	<u>Poor</u> : advanced section loss, deterioration, spalling or scour
3	<u>Serious</u> : loss of section, deterioration, spalling or scour have seriously affected primary structural components; local failures are possible; fatigue cracks in steel or shear cracks in concrete
2	<u>Critical</u> : advanced deterioration of primary structural elements; fatigue crack in steel or shear cracks in concrete; scour may have removed substructure support; may be necessary to close the bridge until corrective action is taken
1	<u>Imminent failure</u> : major deterioration or section loss present in critical structural components; obvious vertical or horizontal movement affecting structure stability; bridge closed to traffic but corrective action
0	<u>Failure</u> : beyond corrective action; out of service

Pontis Model

Pontis is a bridge management software developed by the Cambridge Systematics Inc. for the Federal Highway Administration (FHWA) in the 1990s. The Pontis model, based on simulation of structural deterioration, depicts the bridge as a set of components

(Cambridge Systematics, Inc. 2005; Floyd 2010; Gutkowski and Arenella 1998). In other words, each bridge component (beams, deck, bearings, etc.) is individually modeled and placed together to form the whole bridge system. Some of the inputs used to perform the simulation are: inspection data, preservation policy, budget, deterioration rates, agency costs and user costs (Cambridge Systematics, Inc. 2005). The deterioration rates and costs are entered for each bridge component. Upon entry of the inputs, the model simulates the bridge conditions, develops preservation policy, and makes maintenance and/or repair recommendations for each bridge component (Cambridge Systematics, Inc. 2005). The bridge condition assessment results from Pontis are given in terms of (Cambridge Systematics, Inc. 2005): (1) recommendations for immediate repair needs and future maintenance activities, (2) bridge component conditions, (3) health index and (4) mapping to the National Bridge Inventory (NBI) condition ratings. For the purpose of communicating risk to the general public, each bridge is given an overall rating of sufficient, structurally deficient or functionally obsolete. These condition assessments cover bridge components, bridge systems and bridge networks. The preservation models are developed using historical inspection data and expert opinion, then optimized with cost inputs using a Markovian model (Cambridge Systematics, Inc. 2005; Gutkowski and Arenella 1998; Huang 2010). The recommended maintenance and/or repairs proposed by Pontis are normally compiled and compared with inspector recommendations before a bridge plan is chosen.

ANN Model

The Artificial Neural Network (ANN) model is a forecast model that mimics the biological neural network by adapting and changing as new information is input into the system. The model takes into account multiple parameters, which are previously defined through research and case studies. The parameter model inputs are gathered through inspection reports, Pontis data and inventory data (Huang 2010). Two downfalls of the ANN model are its reliance on good maintenance records and inability to model the relationships between different components.

BRIDGIT Model

BRIDGIT consists of two modules: BRIDGE-1 and BRIDGE-2. BRIDGE-1 is used on-site during inspections to record inspection data and help inspectors make maintenance recommendations. The knowledge-based system diagnoses a problem, identifies its causes, and suggests repair techniques (de Brito et al. 1997). Data from the BRIDGE-1 module is input into the BRIDGE-2 module, which ranks the defined problems based on the safety of the bridge and maintenance policy (de Brito et al. 1997). The same indicators alongside reliability and economic analysis are used to determine maintenance strategies (de Brito et al. 1997). The process used by the BRIDGE-2 module is based off the Markovian model (Huang 2010).

SHM Sensors

Structural Health Monitoring (SHM) sensors continuously monitor the bridge system in real-time. The sensors can be placed in areas of the bridge where degradation can occur but normal inspections techniques cannot access, which allows detection of

internal bridge damage. Detection of the damage is based on changes in the geometry or material properties of bridge components (Farrar and Worden 2007; Worden et al. 2007). The sensor outputs are periodically collected to compare to the historical bridge data, which helps to assess the condition of the bridge (Doebbling et al. 1996).

While SHM sensors allow prediction of the conditions of the bridge system and individual components, its reliance on historical structural responses can make it more difficult to predict during the early years of the bridge's life. It can also be a challenge to determine which structural responses are related to damage so the damage can be properly quantified (Farrar and Worden 2007; Worden et al. 2007). Application of SHM sensors to existing bridges can be difficult or impossible, since a lot of sensors must be placed within bridge components. These types of sensors can only be applied to existing bridges during replacement or retrofitting of bridge components. Application of SHM sensors can also be very costly. Overall, SHM sensors could be a beneficial tool to use, however, it may need to be paired up with a complementary tool to be most effective and cost efficient.

Post-Tensioned Concrete Box Girder Bridge Failure Risk Analysis

Concrete box girder bridges emerged in the United States in the late 1950s. Today they are favored for their quick on-site assembly. There are two main types of concrete box girders (Figure 2-1): (1) adjacent box girders and (2) segmental box girders. The adjacent box girder bridge, which is normally used for bridge spans 30 to 110 feet, consists of multiple box girders of span-length aligned transversely. The box girders are

normally individually prestressed longitudinally and connected to each other transversely through grouted shear keys and post-tensioning tendons. The segmental box girder bridge consists of multiple segments aligned longitudinally across the bridge span. The segmental box girders are connected through shear keys, longitudinal post-tensioning tendons and epoxy-filled joints. Segmental box girders can also be individually post-tensioned transversely. The current design of segmental box girders calls for post-tensioning tendons to be placed in non-degradable ducts filled with grout to help protect the tendons from corrosion. The sealing of the keyways and joints with grout or epoxy helps the adjacent beams/segments to resist against vertical shear forces. Under current practice, shear keys and joints are protected by a waterproof barrier applied on top of the girder system prior to placement of a wearing surface (asphalt or concrete topping); however, some bridges have been constructed without a waterproof barrier. Together the shear keys and post-tensioning tendons enable service loads to be distributed among the adjacent beams/segments.

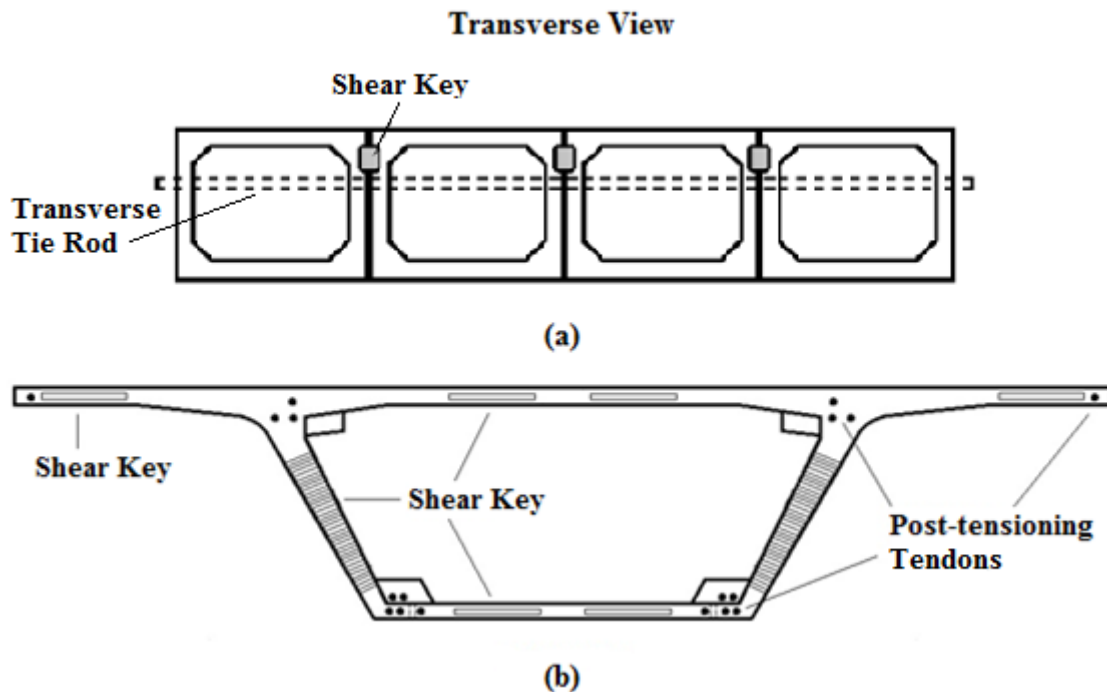


Figure 2-1. Concrete Box Girders: (a) Adjacent (b) Segmental

The problem with concrete box girder bridges is the incline in failures and closures. According to the work of Sharma and Mohan (2011), 21 concrete box girder bridges failed between 1800 and 2009. The failure cases were located in Colorado, Florida, Illinois, Indiana, New York, Ohio, Pennsylvania and Virginia (Naito et al. 2010a; Russell 2009). The leading causes of failure for all bridge types are hydraulic events (54%), collisions (14%), overloading (12%) and deterioration (5%). For prestressed concrete box girder bridges, deterioration seems to have a higher impact on failure, especially in northeastern regions of the United States (Naito et al. 2010a). A survey presented in the National Cooperative Highway Research Program (NCHRP) Synthesis 393 on Adjacent Precast Concrete Box Beam Bridges: Connection Details (Russell

2009), showed the skew of the bridge, presence of topping, performance of the waterproof membrane, and bridge maintenance are the four key factors thought to have the most influence on the long-term bridge performance. The survey results also found longitudinal cracking along the grouting of adjacent beams and leakage of water and chlorides through joints to be the two most common problems observed (Russell 2009).

Some of the failure modes that are particular to adjacent box beams, are: waterproofing membrane, concrete, shear key and prestressed/post-tensioned tendon failures. The main cause of waterproofing membrane failure is large beam displacements due to overstressed/overloaded beams (MDOT 2005). Overstressing of beams can also cause cracking of the concrete. Other causal factors are temperature variants, insufficient reinforcement, premature releasing of prestressing strands during curing, loss of prestress, concrete shrinkage during curing and concrete deterioration (MDOT 2005). The cracks expose the interior concrete and grout to water, chlorides (deicing salts) and acidic gases (e.g. CO₂), which cause deterioration. At this stage, shear key failure can occur due to deterioration of the shear key grout. In addition to shear key failure, the deterioration eventually leads to corrosion of tendons. Most post-tensioning tendon corrosion is localized at joints, shear keys and anchorage areas, where water and chlorides have easier access to the post-tensioning reinforcement (MDOT 2005). It may be noted that the occurrence of any one of these failures increases the likelihood of one of the other failures occurring. For example, failure of the waterproofing membrane provides access for water and chlorides to penetrate into the shear key and concrete

deteriorating the grout and concrete, which eventually leads to the corrosion of reinforcement/tendons.

For segmental box girders, the same types of failure can occur, however there are some differences in post-tensioned tendon failure. In current practice, post-tensioned tendons are placed in grouted, non-degradable ducts, which provide an extra barrier for the water and chlorides to penetrate. Once the water and chlorides get through the segmental joints, they can enter through splits in the duct sleeves, unsealed duct joints and unsealed grout inlets/outlets used for placement of grout inside the ducts (Corven and Moreton 2004). Once the water and chlorides get into the duct, they begin to degrade the grout and corrode the tendons. Bridges built during the early stages of post-tensioning were often constructed with post-tensioning tendons inside the concrete with non-degradable duct material and no grout, because the sole purpose of the duct was to form a void in the concrete for the tendons to go through (Corven and Moreton 2004). This construction method allowed chloride-water quicker access to the tendons. A second mode of failure risk exists for grouted ducts. If the duct is not properly grouted, accumulation of bleed water can cause corrosion of the tendons and create voids in the grout (Corven and Moreton 2004).

These failure modes are just a few of the ways failure can occur. Several other factors contribute to the failure of a bridge. One failure mode known to occur for all types of bridges is scour, which is the result of flowing water eroding the abutment or pier foundation. When scour reduces the foundation depth enough that vertical movement is allowed, failure can occur (Johnson 1999; LeBeau and Wadia-Fascetti

2007). The following case study of the Lake View Drive Bridge shows some other common failure modes seen by box girders.

Lake View Drive Bridge Failure Case Study

In December 2005, the Lake View Drive Bridge in Washington County, Pennsylvania collapsed due to internal deterioration of reinforced concrete beams. The bridge was a four-span prestressed adjacent box girder bridge constructed in 1960. Some of the design and construction problems that help to accelerate the deterioration were: (1) the absence of a waterproof barrier on the deck, (2) the absence of grouting in the shear key, (3) open vent holes, (4) open void area, (5) inadequate development length of reinforcement and (6) inadequate reinforcement coverage due to movement of void forms (Harries 2009; Naito et al. 2010b). The open vent holes used during construction for curing the concrete and the open void form allowed chloride-saturated water to enter the box girder void. The water degraded the cardboard void form, which clogged the void drain hole and allowed the water to sit inside the beam (Naito et al. 2010b). By allowing the chloride-saturated water to sit inside the beam for an extended amount of time, the corrosion of the interior reinforcement was accelerated. Perhaps, if the drain had been larger allowing the material and water to exit the beam, the corrosion would not have been so extreme. Together, these defects resulted in the collapse of an inner span exterior beam.

Changes in Design and Construction Procedures

Some of the failures discussed have been prevented or improved through changes in design and retrofits. In the 1970s, failure was seen to occur due to deterioration from

top to bottom flange; therefore, in the 1980s, construction involved a waterproof barrier being laid prior to the placement of the wearing surface (Naito et al. 2010a). The typical size and placement of void drains became more consistent with two-inch diameter drains placed every 10 to 15 feet along the beam (Corven and Moreton 2004). For adjacent box girder bridges, void forms changed from open and degradable forms to closed-cell polystyrene forms (Naito et al. 2010b; Russell 2009). In the construction of segmental concrete box girder bridges, degradable duct material was replaced by non-degradable material. Some of the non-degradable and corrosion resistant materials used are galvanized steel, stainless steel, polyethylene plastic, polypropylene plastic or high density polyethylene. In addition to helping prevent penetration of water, the high density plastics also provide better protection from chloride ions (Corven and Moreton 2004). Even though these actions have been taken, the related failure modes should not be ignored.

Fault-Tree Analysis (FTA) as a Risk Assessment Tool

H. A. Watson of Bell Laboratories, who was assigned by the United States Air Force to assess the Minuteman Launch Control System, developed FTA (Ericson 1999). FTA, a risk assessment tool, consists of two types of analysis: qualitative and quantitative. Qualitative analysis involves developing a visual model of events leading to failure and their relationships. Each event leading to failure is connected by an OR, AND, EXCLUSIVE OR, INHIBIT and PRORITY AND gate. The events that make up the fault-tree are classified as intermediate, basic, undeveloped, conditional or house

events. Figure 2-2 and Figure 2-3 show the gate and event symbols along with their descriptions.


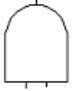

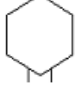

	Gate Name	Description
	OR	Output event occurs if one of the input events occurs
	AND	Output event occurs if all the input events occurs
	EXCLUSIVE OR	Output event occurs if one but not both of the input events occurs
	INHIBIT GATE	Output event occurs if a single input event and a conditional event occur
	PRIORITY AND	Output event occurs if all input events occur in a specific sequential order

Figure 2-2. Fault-Tree Gate Symbols and Descriptions

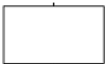
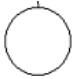



	Event Name	Description
	INTERMEDIATE	An event that results from one or more preceding events acting through logic gates
	BASIC	Initiating event which cannot be further developed
	UNDEVELOPED	An event that cannot be further developed due to insufficient information
	CONDITIONAL	A specific condition applied to an INHIBIT or PRIORITY AND gate
	HOUSE	An event which is expected to occur or not occur

Figure 2-3. Fault-Tree Event Symbols and Descriptions

In FTA, cut sets are used to describe unique combinations of events that cause the top event to occur. Minimal cut sets are those combinations that have the shortest path to the

top event. Quantitative analysis is performed by applying probabilities to all basic, undeveloped, conditional and house events and using Boolean algebra and probabilistic mathematics to solve for the occurrence probability of the top event and minimal cut sets. The analysis results aid in the decision-making process for application of countermeasures.

It was the unique combination of the qualitative and quantitative analysis that gave FTA its advantage as a risk assessment tool. Dave Haasl of Boeing Company recognized the implication of FTA as a risk analysis tool and led the application of FTA to the entire Minuteman Missile System in 1964 (Ericson 1999). A couple years later, in 1966, Boeing began using FTA in their commercial aircraft design process (Ericson 1999).

It was Boeing Company that began trying to improve FTA, which they did through the development of a 12-phase simulation program (Ericson 1999). However, FTA soon entered the nuclear power industry, who is accredited for most of the major improvements made to FTA. In 1981, the Nuclear Regulatory Commission published the *Fault Tree Handbook* (Haasl et al. 1981). The nuclear power industry made most of its changes to the algorithms and codes used to run FTA. Improvements were also made through application of FTA to catastrophic accidents, such as the NASA Apollo 1 launch pad fire on January 27, 1967, the Three Mile Island nuclear power plant accident on March 18, 1979 and the NASA Challenger Space Shuttle accident on January 28, 1986 (Ericson 1999). The majority of the improvements occurred between 1981 and 1990,

during which time FTA began to get international recognition and began its entry into safety software (Ericson 1999).

Over the years, FTA has entered into several industries, such as chemical process, auto, rail transportation and robotics. Within these industries, it has been used for a variety of assessments – “numerical requirement verification, identification of safety critical components, product certification, product risk assessment, accident/incident analysis, design change evaluation, visual diagrams of cause-consequence events and common cause analysis” (Ericson 1999).

Summary and Discussion

While each of the current risk assessment methods has benefits, they also have some limitations. For the risk assessment methods reviewed, limitations observed in one or more methods were:

- Inability to assess the condition of internal components (e.g. visual inspection)
- Requirement of a significant amount of technical data for analysis (e.g. ANN model)
- No identification of the chain of events leading to bridge failure
- Assessment of individual component conditions instead of individual component and whole bridge system conditions

FTA is tool that has been used for risk assessment of products in a variety of industries over the last 37 years. Some of the industries have applied the risk assessment prior to the occurrence of failure, while others have used it post-failure to determine the likely

cause of failure. Currently, FTA is not used as a risk assessment tool to prevent bridge collapse. For this research, the application of FTA to bridge failure will be assessed. Since the qualitative and quantitative assessments used in FTA address many of limitations of the risk assessment methods reviewed and it has been successfully used in a variety of industries, its application to bridge failure is expected to be beneficial. To test the applicability of FTA as a tool for risk assessment of bridge failure, case studies were conducted on post-tensioned concrete box girder bridges. Post-tensioned concrete box girder bridges were chosen due to the number of closures and collapses that have occurred over their relatively short lifetime of approximately 50 years. The bridges have a history of bridge collapse due to internal failures, which allowed the use of FTA to analyze internal components to be assessed. The process and methods used to perform FTA on bridges is discussed in the Chapter 3.

CHAPTER THREE

RISK ASSESSMENT PROCESS AND METHODOLOGY

The first step in risk assessment is to research and identify plausible causes of bridge failure for the bridge type of interest, which helps to develop the qualitative structure of the fault-tree. Once the qualitative part of the fault-tree is developed, minimal cut sets can be identified and occurrence probabilities can be assigned to basic events. Identification of the minimal cut sets with the highest probability of failure allow for prioritization of countermeasures.

Fault-Tree Development

Before the fault-tree can be qualitatively developed, technical knowledge of the bridge and its structural components is necessary. In addition, a list of plausible failures and their causes must be compiled. Expert opinion, failure case studies, inspection reports are a few sources that can be used to find this information.

Once the different failure components and causes have been identified, the fault-tree can be developed. The fault-tree starts with the top event, bridge failure, and is broken down into primary bridge components that can lead to bridge failure if the component fails. Each component is then broken down into events that can directly lead to the component failure. The appropriate gate is chosen to link each primary component event to their causal events. The cause-and-effect process continues until none of the

events can be broken down further. The bottom events are then defined as basic, undeveloped or house.

A fault-tree does not have to contain all events that could possibly occur; rather, it only needs to include events that could occur within reason. If the event has not previously shown to be a plausible initiating event with similar bridges then, the event may be excluded. A common rule is to use the minimum necessary number of events. Another common practice is to avoid using the same event more than once because the event is counted in the analysis as many times as it occurs, which results in biased quantitative results. To avoid duplication of an event, such as a collision, that can affect multiple bridge components, be more specific in identifying the event (i.e. specifying the component affected).

Minimal Cut Sets

Minimal cut sets are the shortest combination of events leading to the top event. These combinations are found using Boolean algebra. In this study, minimal cut sets were calculated using Isograph FaultTree+ software (Figure A-1) (2008). A variety of fault-tree software are available for constructing fault-trees and computing their cut sets.

Occurrence Probabilities

The sources that can be used to estimate the occurrence probabilities of the fault-tree basic events are: public databases, experimental data, model analysis, expert opinion and published research findings. Most of the time, probabilities found in these sources

are not directly applicable to the basic event; therefore, statistical and probabilistic analysis must be used to estimate the occurrence probabilities of the basic events. The procedure used to develop the final basic event probabilities from published findings is discussed in the following example.

Consider an example where concrete deterioration and corrosion is an initiating failure event. For this example, the probability was calculated using data from two studies (Wardhana and Hadiprono 2003, Sharama and Mohan 2011) on bridge failures in the U.S. Table 3-1 shows the average number of bridges and number of failures due to concrete deterioration and corrosion for each surveyed period. The average number of bridges in a given period was calculated using data from previous studies and the NBI Database (FHWA 2011). All the data collected were used to develop the annual probability of failure of all the bridges in the U.S. due to concrete deterioration and corrosion. The equation used to estimate the annual probability of failure was:

$$P_{f,N} = 1 - (1 - P_{f,A})^N \quad (3-1)$$

where, $P_{f,N}$ is the probability of failure for given period range, $P_{f,A}$ is the annual probability of failure, and N is period range in years. It should be noted that Equation 1 assumes the annual concrete deterioration and corrosion failure probabilities are independent and uncorrelated from year to year. This assumption is not entirely true since the failure probability will vary over time as deterioration occurs or maintenance is performed. For simplicity, it is assumed that major maintenance is not performed over the considered time period. Thus, the annual failure probability can be modeled as an identical and independently distributed variable. Solving for $P_{f,A}$, the equation becomes:

$$P_{f,A} = 1 - (1 - P_{f,N})^{(1/N)} \quad (3-2)$$

The annual probability of bridge failure due to concrete deterioration and corrosion calculated for each study can be seen in Table 3-1. The average annual probability calculated can then be input into the fault-tree.

Table 3-1 Bridge Failures Due to Concrete Deterioration and Corrosion					
Period	Period Range (Years)	Avg. No. of Bridges	No. of Failures	$P_{f,N}$	$P_{f,A}$
1989-2000	11	592,966	1	1.69e-06	1.53e-07
1800-2009	209	600,119	8	1.33e-05	6.38e-08
				Average	1.09e-07

Structural Health Monitoring Countermeasures

To prioritize implementation of countermeasures, the minimal cut sets must be identified. Once the minimal cut sets are identified, historical data on bridge failures can be used to develop probabilities for the occurrence of the cut sets. Countermeasures that are expected to have the largest impact on the health of the bridge should be implemented. In some cases, one countermeasure may be applied to a bridge to reduce the occurrence of multiple causal factors. One type of countermeasure that can be used is SHM sensors. Intelligent sensors installed on a bridge, act as a warning system by alerting the infrastructure manager when events that could lead to bridge failure are detected. The warning system allows infrastructure managers to prevent the event from progressing by planning for maintenance activities to fix the problems. As a result, the risk of bridge failure is reduced.

The expected reduction in the probability of bridge failure can be calculated by including the sensors in the fault-tree. Take an example where the annual probability of bridge failure due to scour is $4.61e-06$. After 30 years, the expected probability of failure increases to $1.38e-04$. In attempts to reduce the probability of failure due to scour at 30 years, Time Domain Reflectometry (TDR) will be applied to the bridge to monitor the foundation depth. If the foundation depth becomes increasingly low, a warning will be sent to the bridge manager, who will take remedial actions. As with any technology, TDR is not 100% accurate. Four outcomes must be considered (Figure 3-1): 1) positive detection, 2) false positive detection, 3) negative detection, and 4) false negative detection.

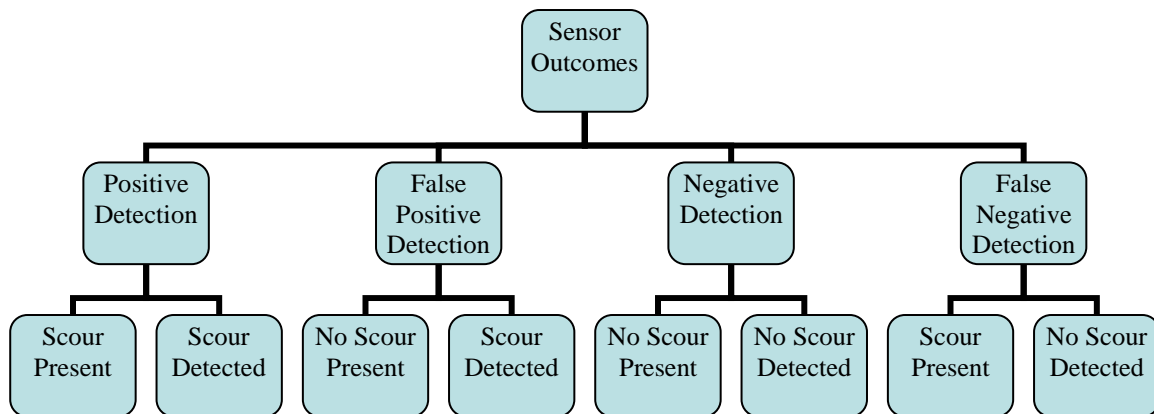


Figure 3-1. Sensor Detection Outcomes

TDR is expected to result in error 5% of the time. Since the probabilities input into the fault-tree are the probabilities of bridge failure, the probability of false negative sensor detection needs to be incorporated into the fault-tree. For illustration purpose, a value of 0.05 is used for the probability of false negative TDR sensor detection. The new probability of failure due to scour is the result of TDR not detecting scour and scour

being advanced enough to cause bridge failure. Figure 3-2 shows how the sensor is applied to the fault-tree model and the resulting new probability of bridge failure.

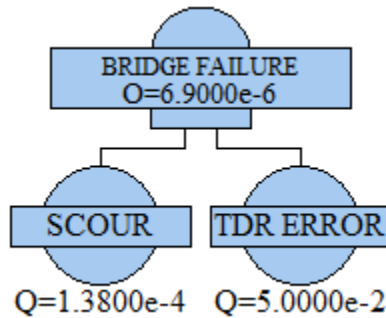


Figure 3-2. Bridge Failure Due to Scour and Sensor Failure

Case Studies

The first study is the development of a qualitative fault-tree analysis (FTA) model for adjacent concrete box girder bridges. The second study is a complete FTA of a particular bridge to determine its failure modes, risk of failure, and plausible countermeasures.

Post-Tensioned Adjacent Concrete Box Girder Bridges

Adjacent concrete box girders are typically prestressed longitudinally. Prestressing strands are created by pulling strands in tension prior to placement of concrete so the concrete can cure directly against the tensioned strands. The manufactured beams are transported to the construction site for placement, where they are tied together. They are usually tied together with grouted shear keys and transverse steel rods or post-tensioned strands. The solid connection of the shear keys and lateral ties enable the service loads to be distributed among the adjacent girders. On top of the

girder system, either a wearing surface is directly applied or a waterproof barrier is laid prior to placement of the wearing surface.

James B. Edwards Bridge in Charleston, SC

The James B. Edwards Bridge of Charleston, SC (Figure 3-3) constructed in 1989 consists of two post-tensioned side-by-side concrete segmental box girders. The bridge services a section of I-526, which crosses over the Wando River (salt water), and two two-lane roads (one at each end of the bridge). Since the bridge crosses the Wando River closer inland, there is minimal commercial vessel traffic beneath the bridge. The two-lane underpasses are also lightly traveled. There have not been any collisions to the piers noted. Problems that have been identified through inspections by the SCDOT are (Figure 3-4): 1) improper grouting of ducts, 2) leaky joints, 3) debris in the box void, 4) clogged void drain holes (3/4-inch diameter) and 5) cracks in the piers. Additional pictures of the bridge can be seen in Appendix C.



Figure 3-3. James B. Edwards Bridge of Charleston, SC



Figure 3-5. SCDOT Inspection of James B. Edwards Bridge: (a) Improper Grouting of Ducts (b) Small Void Drain Holes (c) Cracks in Piers (d) Leaky Joints

CHAPTER FOUR

CASE STUDY: FAULT-TREE QUALITATIVE ANALYSIS FOR POST-TENSIONED ADJACENT CONCRETE BOX GIRDER BRIDGES

Fault-Tree Development

Failure of a bridge (system failure) is usually initiated by failure of key superstructure or substructure components, such as the beams, abutments, piers, bearing pads and foundation. Beam collapse is due to overloading by high traffic loads or overweight trucks, reduced strength from extreme heat, collisions, and corrosion of reinforcement and post-tensioning tendons. Foundation failure is the result of scour, which is caused by water flow eroding the foundations. When the foundation depth is shallow enough that the abutment or pier can move vertically, failure can occur (LeBeau and Wadia-Fascetti 2007). The major cause of bearing failure is extreme lateral forces that knock the superstructure off the bearings (LeBeau and Wadia-Fascetti 2007). The extreme lateral forces can come from environmental or collisions events. The collision events can also cause local damage to abutments or piers, which can result in failure. Another source of abutment and pier failure is corrosion. The events leading to superstructure and substructure failure can be seen in Figures 4-1 and 4-2, respectively. It should be noted that the green colored events in the figures are the basic and undeveloped events.

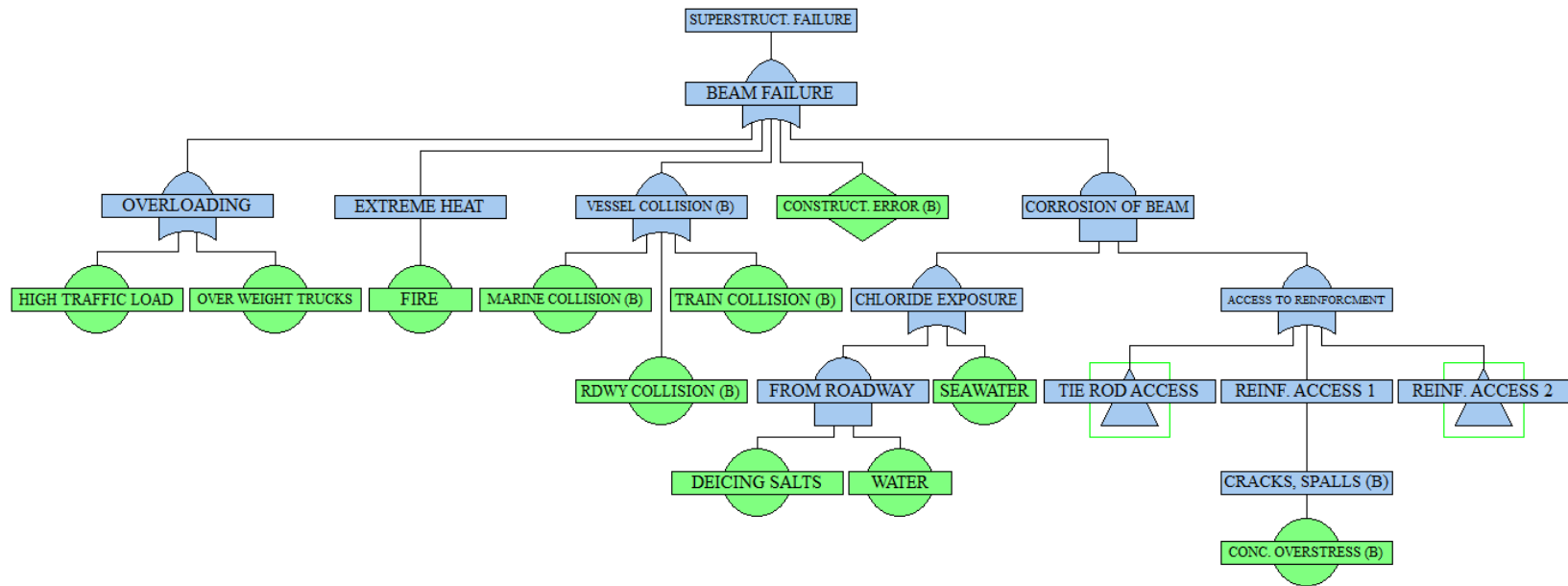


Figure 4-1. Fault-Tree Model for Superstructure of Adjacent Box Girder Bridges

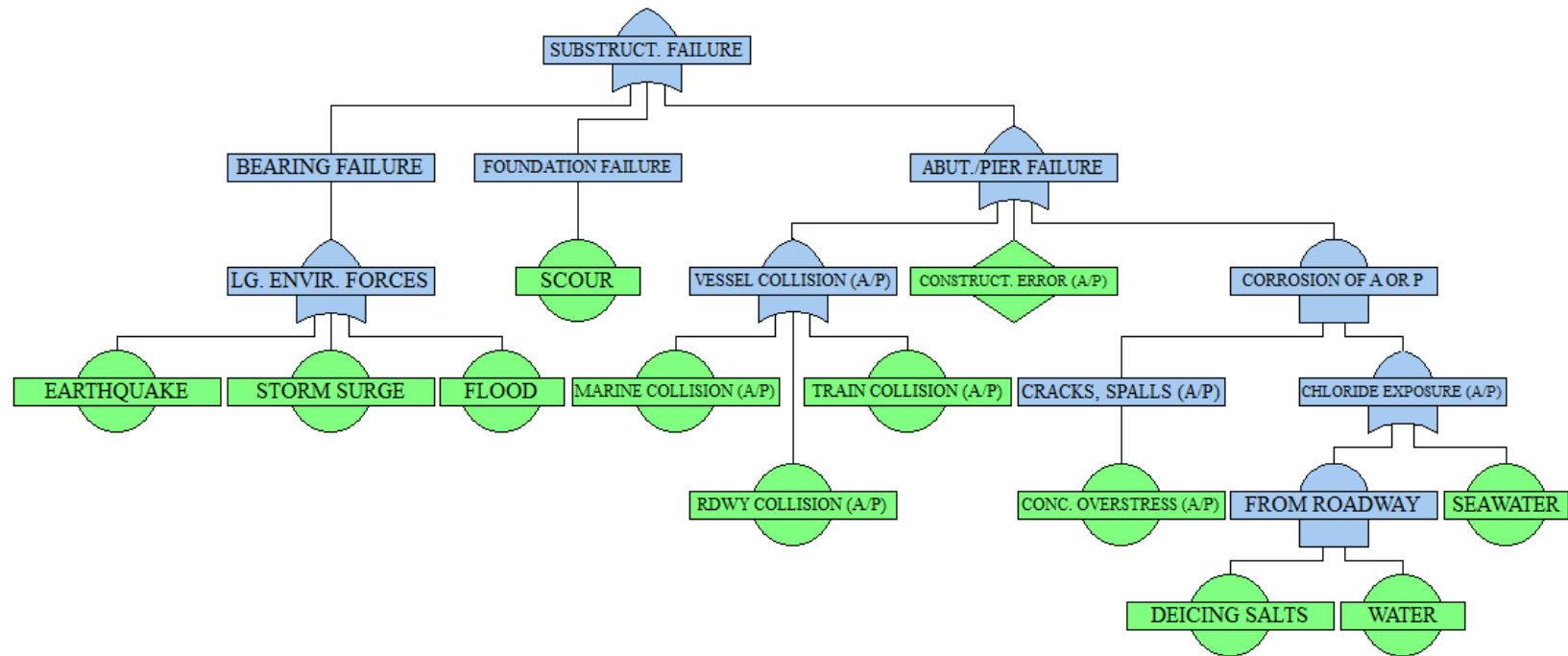


Figure 4-2. Fault-Tree Model for Substructure of Adjacent Box Girder Bridges

Superstructure Failures

Over time, the amount of traffic that bridges must handle can increase beyond the design capacity, which leads to overloading of the girders. The girders can also be overloaded due to reduction of girder strength. The capacity of a girder can be reduced by temperatures above the 120°F maximum design temperature. This phenomenon has been defined as extreme heat in the fault-tree (LeBeau and Wadia-Fascetti 2007). Collisions and corrosion also have an effect on the beam strength. Collisions refer to marine vessels, trucks, or trains producing large impact forces on the girders, which are a result of height limit violations, accidents or intentional attacks. Corrosion occurs when water with high chloride concentrations have access to reinforcement and interact with the iron in the strands (Sianipar and Adams 1997). The chloride-water can come from sea water or deicing salts mixed with wet weather conditions (i.e. snow, ice, rain).

The main entry point for chloride-water to tie rods is through cracks in the concrete, waterproof barrier and keyway sealant, which are initiated by overstressed girders undergoing large displacement (MDOT 2005). A waterproof membrane that is defective or non-existent allows chloride-water to reach the underlying concrete and keyways. When the chloride-water enters the grouted keyways, it flows through cracks and further deteriorates the grout. In some instances, grouting is not properly executed during the construction phase, which allows larger amounts of water to pass through. Once the water passes through the keyway, it comes in contact with the tie rods, which are placed directly below the keyway, and begins the corrosion process. Figure 4-3 shows the fault-tree developed to depict the tie rod access points.

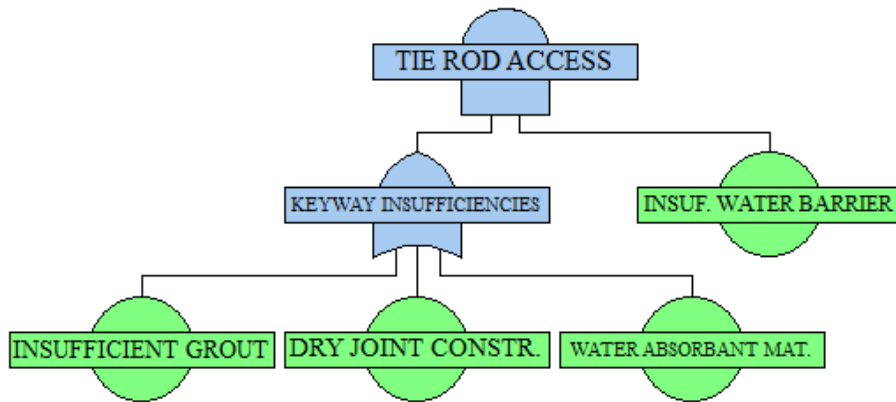


Figure 4-3. Fault-Tree Model for Tie Rod Access

Key entry points to reinforcement are cracks in the concrete, insufficient concrete cover, and unsealed vent holes. Unsealed vent holes accompanied by an open void form allows for the chloride-water to enter the box void. When the roadway slopes toward the vent holes and a curb is in place, the amount of water that gains access to the vent holes is even greater. Once the water enters the void, it interacts with the form and, if the form material is degradable, the form breaks apart and makes its way to the drains. If the drain holes are not large enough, then the material clogs the drain allowing the chloride water to sit in the void and penetrate the internal concrete. When this happens, not only is the loading imposed on the superstructure increased, the corrosion process is expedited (Sianipar and Adams 1997; Naito et al. 2010). This succession of events was developed into the fault-tree shown in Figure 4-4.

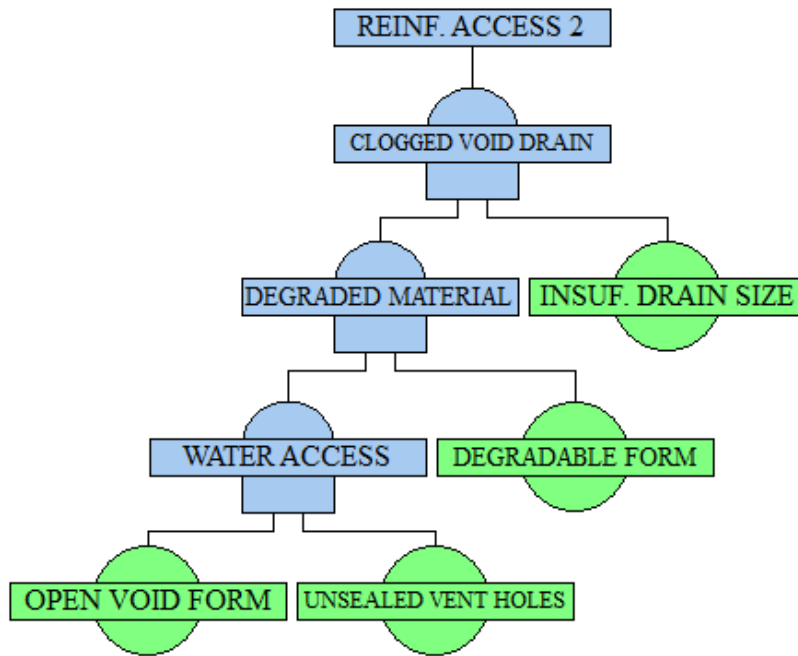


Figure 4-4. Fault-Tree Model for Reinforcement Access

Substructure Failures

Foundation failure is due to scour, which can be characterized as one of the following: 1) contraction scour, 2) local scour, 3) degradation, 4) channel widening and 5) lateral migration (Johnson 1999). The causes of contraction and local scour, respectively, are flow constrictions and obstruction in the flow due to bridge substructure. Degradation, channel widening and lateral migration are natural occurring events. Degradation affects the foundations by lowering the entire channel bed. Channel widening and lateral migration has greater affects on the abutments and piers that were not designed to be exposed to the channel flow. The amount of scour present depends on several factors, such as the flow characteristics, channel dimensions and material properties.

Environmental events with large lateral forces, such as storm surges, floods and earthquakes have been stated to cause bearing failure (LeBeau and Wadia-Fascetti 2007). The extreme lateral forces seen by collisions can cause bearing failures, as well as, abutment and pier failure. The bearing failure is due to misalignment of bearing pads and abutment and pier failures are due to severe local damage of the components. Abutment and pier failures can also be the result of corrosion, which can occur when chloride-water enters cracks in the abutments or piers or penetrates through the concrete cover. The concrete cover can be penetrated when insufficient cover is provided during construction. These events were depicted in the Figure 4-2.

Minimal Cut Sets

The minimal cut sets that appear to be most influential to the complete adjacent box girder bridge fault-tree, shown in Figure B-1, are:

- High Traffic Load
- Over Weight Trucks
- Fire
- Marine Collision with Beam
- Roadway Collision with Beam
- Train Collisions with Beam
- Construction Error in Beam
- Earthquake
- Storm Surge

- Flood
- Scour
- Marine Collision with Abutment or Pier
- Roadway Collision with Abutment or Pier
- Train Collisions with Abutment or Pier
- Construction Error in Abutment or Pier

These minimal cut sets are the most critical because they have the least number of events leading to the top failure. For this fault-tree qualitative analysis, all the most influential minimal cut sets are single-event cut sets. The most influential cut sets could change with quantitative analysis. The complete list of minimal cut sets is provided in Appendix B.

CHAPTER FIVE

CASE STUDY: FAULT-TREE ANALYSIS FOR JAMES B. EDWARDS BRIDGE

Fault-Tree Development

Superstructure Failures

The primary reasons for chloride-water in segmental concrete box girder bridges, such as the James B. Edwards Bridge, are insufficiencies in the concrete, waterproof barrier and keyway sealant. These key factors are similar to those discussed for adjacent concrete box girder bridges in Chapter 4. Once chloride-water passes through the waterproof barrier, it enters the segmental joints. The James B. Edwards Bridge has wet joints, which are joints sealed with a material such as grout or epoxy. When the sealant has cracks, chloride-water flows through the cracks and further deteriorates it allowing water to flow completely through the joint and enter the girder void. Two concerns with chloride-water entering the void are: 1) internal reinforcement corrosion (as discussed in Chapter 4) and 2) post-tension tendon corrosion. Tendon corrosion starts when the water in the void comes in contact with interior ducts. Water can enter the ducts through splits, unsealed joints or unsealed grout inlets/outlets (Corven and Moreton 2004). Water inside the duct degrades the surrounding grout allowing direct access to the post-tensioning tendons. Often, the ducts are not properly grouted during construction, which allows water from grout bleeding or external sources to have more direct access to the tendons. The fault-tree developed for the superstructure is shown in Figure 5-1. The corrosion processes are depicted as undeveloped events for quantitative analysis purposes.

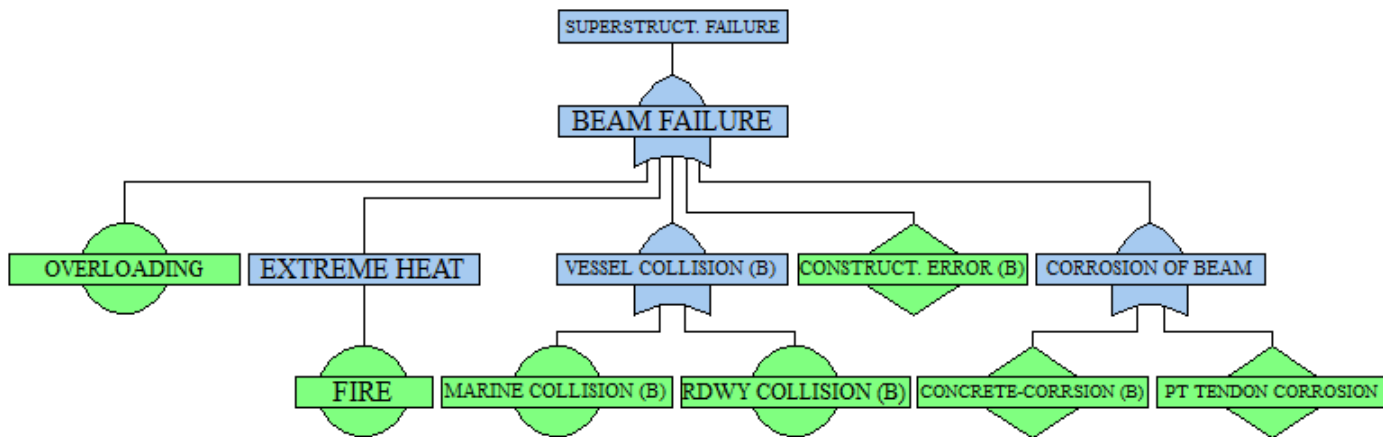


Figure 5-1. Fault-Tree Model for James B. Edwards Bridge Superstructure Failure

Substructure Failures

The substructure failures for the James B. Edwards Bridge are the same as those described for the Adjacent Concrete Box Girder in Chapter 4 except for train collisions, which are not considered in the FTA. The final substructure fault-tree can be seen in Figure 5-2. For quantitative assessment purposes, the fault-tree depicts the concrete-corrosion event as an undeveloped event.

Minimal Cut Sets

Each of the minimal cut sets for the James B. Edwards Bridge fault-tree (Figure C-9) are single-event cut sets; therefore, each basic event is considered equally influential to the top event, bridge failure. The minimal cut sets are listed in Appendix C. In the next section, quantitative analysis will be performed to rank the minimal cut sets according to their probability of occurrence.

Occurrence Probabilities

The sources used to develop probabilities for fault-tree events were: 1) studies on bridge failures, 2) bridge inspection reports and 3) expert opinion. The work of Harik (1990), Wardhana and Hadiprono (2003) and Sharma and Mohan (2011) were consulted for analysis of bridge failures in the U.S. Information on post-tensioned tendon failure was gathered from Woodward (2001). A compilation of the data used for development of annual probabilities can be seen in Table C-1. Prior to calculating the annual probabilities, each event was assumed to follow a certain trend. For this fault-tree, the

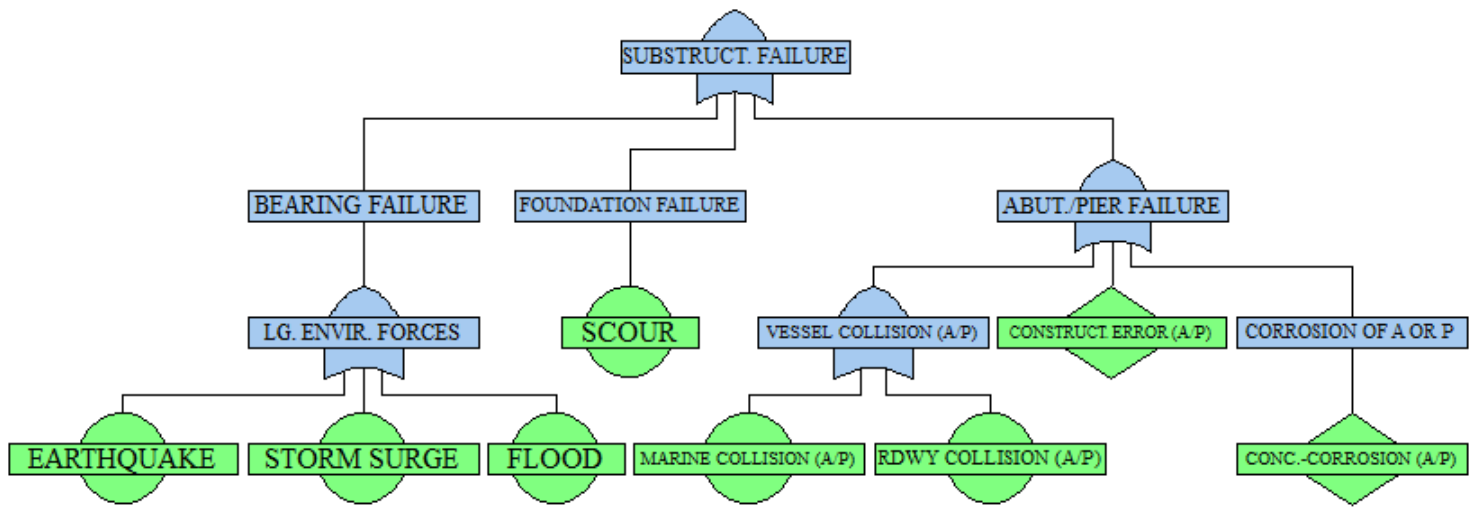


Figure 5-2. Fault-Tree Model for James B. Edwards Bridge Substructure Failure

occurrence probability of each event was assumed to be either constant, for a time invariant event (e.g. construction error), or follow Equation 3-2. The annual failure probabilities, $P_{f,A}$, were estimated using the procedure discussed in Chapter 3 using published failure statistics. Constant trends were calculated by taking the average of the $P_{f,N}$ values. Since some of the data, such as roadway collision, were not broken down into the components (i.e. beam or pier) they affect, resulting probabilities were divided among the components based on field observations of the James B. Edwards Bridge. The trend, ratio, and annual probability for each basic event are given in Table 5-1. Note that “B” refers to beam and “A/P” refers to abutment or pier.

Table 5-1. Annual Failure Probabilities Used for Fault-Tree Analysis			
Failure Mode	$P_{f,A}$	Reference*	Trend Notes
Construction Error (A/P)	2.60e-05	2,3	Constant
Construction Error (B)	2.60e-05	2,3	Constant
Earthquake	1.38e-06	2,3	Equation 3-2
Fire	3.90e-05	1,2,3	Equation 3-2
Flood	1.04e-05	1,2,3	Equation 3-2
Marine Collision	4.36e-05	1,2,3	Constant
Marine Collision (A/P)	1.63e-07		0.75 of Marine Collision
Marine Collision (B)	5.43e-08		0.25 of Marine Collision
Overload	3.18e-06	1,2,3	Equation 3-2
PT Tendon Corrosion	2.40e-06	4	Equation 3-2
Reinforcement Corrosion	1.09e-07	2,3	Equation 3-2
Roadway Collision	6.64e-05	1,2,3	Constant
Roadway Collision (A/P)	1.73e-07		0.40 of Roadway Collision
Roadway Collision (B)	2.61e-07		0.60 of Roadway Collision
Scour	4.61e-06	1,2,3	Equation 3-2
Storm Surge	2.17e-07	2,3	Equation 3-2
* 1. (Harik 1990) 2. (Sharma and Mohan 2011) 3. (Wardhana and Hadiprono 2003) 4. (Woodward 2001)			

The NBI data for North Carolina, South Carolina and Virginia were used to compare the deterioration rates of segmental bridges to all bridge types (Figures 5-3). In Figure 5-3, the numerous ratings of 9 near the end of the bridge design life are a result of maintenance and repairs completed on bridges; therefore, the estimated median deterioration rate also includes maintenance and repair activities. The process used for fitting the median estimate curve to the NBI data is described in Appendix D. The comparison was used to make any necessary adjustments to the probabilistic data that was representative of all bridge types. The initial median superstructure ratings were approximately the same but by the age of 50 there was a difference of approximately one rating unit, which indicates a small variation in the deterioration rates of the superstructures. The superstructure deterioration rate of segmental bridges was larger than the average of other bridge types. The median substructure ratings remained approximately the same throughout the 50 years. Due to the small differences between the superstructure and substructure ratings, no adjustments were made to the calculated basic event probabilities.

Infrastructure safety is often measured in terms of a structural reliability index, β , which is defined by:

$$\beta = \Phi^{-1} (1 - P_f) \quad (5-1)$$

where $\Phi^{-1}(\cdot)$ is the inverse function of the standard normal cumulative density function (CDF) and P_f is the probability of failure. A beta value of 3.1 has been accepted by the International Organization for Standardization (ISO) as the target reliability index under

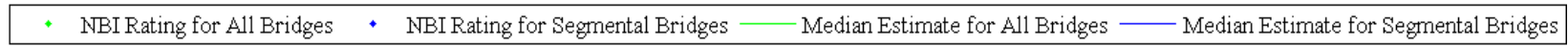
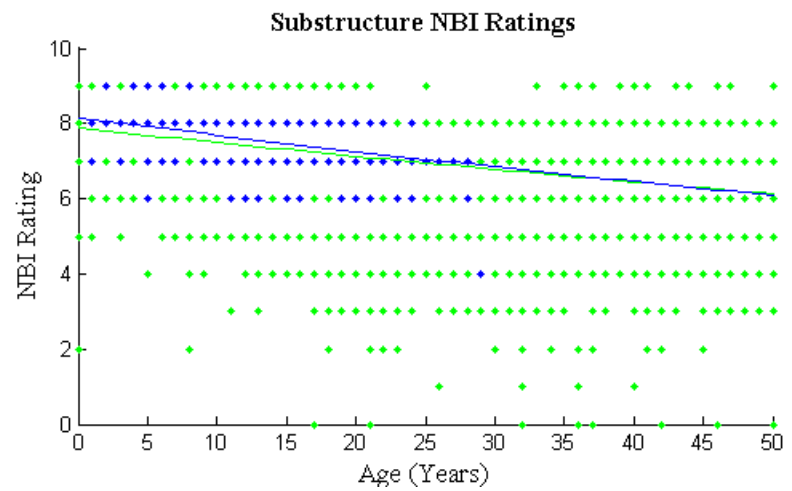
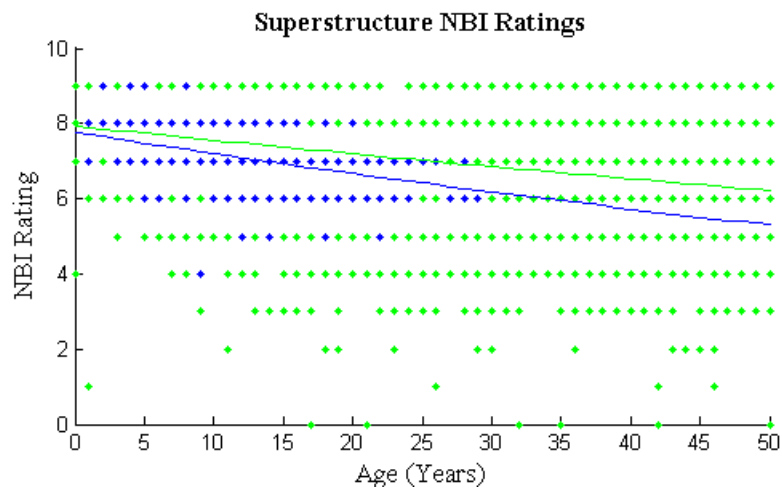


Figure 5-3. NBI Rating Comparison of Segmental Bridges and All Bridge Types

ISO 2394 (1998); therefore, a bridge with a beta value less than 3.1 is considered structurally unsafe. The equivalent probability of failure is 1.00e-03, where a probability of failure greater than 1.00e-03 is considered unsafe.

Since the bridge is currently in service and considered safe by the SCDOT, the fault-tree result for bridge failure at 22 years of age was expected to be less than 1.00e-03. At the age of 50, the fault-tree result for bridge failure was expected to be close to 1.00e-03, since bridges usually have a design life of 50 years. The fault-tree results were as expected with a failure probability of 5.85e-04 at 22 years of age and 1.21e-03 at 50 years of age. Figure 5-4 shows the FTA results for the probability of bridge failure and the corresponding reliability index over the expected lifetime of the bridge, which were computed by solving the fault-tree at each year.

In order to determine the minimal cut sets with the highest risk of failure, probabilities were calculated for each minimal cut set. The top five cut sets based on the calculated probabilities can be seen in Table 5-2. A ranking of all the minimal cut sets and their probabilities can be found in Table C-2.

Table 5-2. Top Five Minimal Cut Sets Based on Probability of Occurrence		
Minimal Cut Set		Probability of Occurrence at Age 50
1	Flood	5.20e-04
2	Scour	2.30e-04
3	Overload	1.59e-04
4	PT Tendon Corrosion	1.20e-04
5	Earthquake	6.91e-05

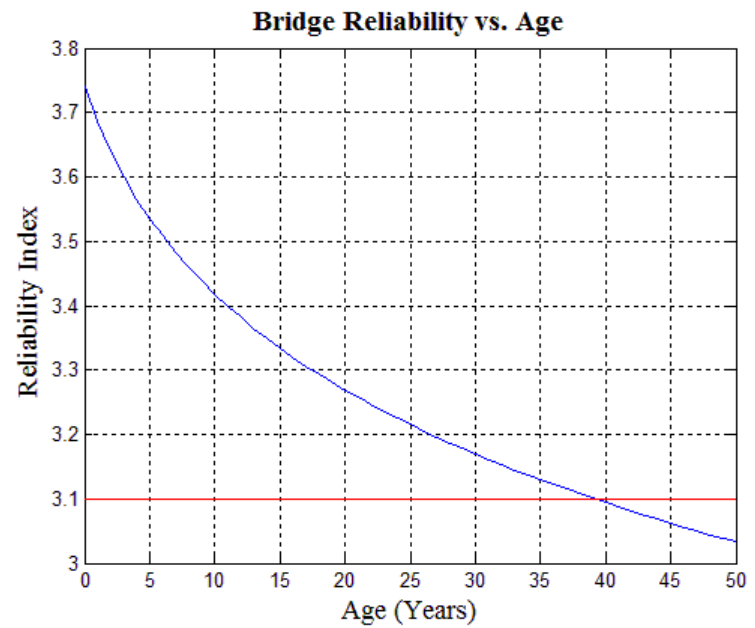
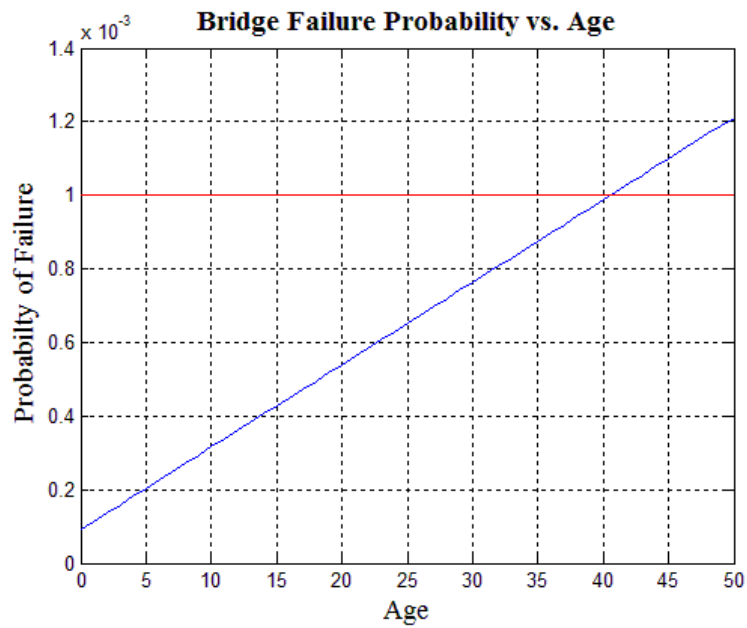


Figure 5-4. Failure Probability and Reliability Index versus Age of the James B. Edwards Bridge

Countermeasures

To identify and implement the most beneficial and cost-effective countermeasure options, the countermeasures should be focused on the most influential minimal cut sets based on failure probability. For this case study, implementation of SHM sensors was considered. Examples of SHM sensors that could be applied to the top five minimal cut sets are listed in Table 5-3. While some of the minimal cut sets, such as an earthquake, are impossible to prevent, SHM sensors can also be used to monitor the effects of an event to determine the safety of the bridge. A list of SHM sensors for all applicable basic events is in Table C-3. An example of how a sensor/countermeasure would be added to the fault-tree for analysis is shown in Figure C-12. For the example, TDR was applied to scour.

Table 5-3. Examples of SHM Sensors for Top Five Minimal Cut Sets		
Minimal Cut Set	SHM Sensors	Ref*
Flood	Accelerometers	2,3,5
	Velocity Transducers	2
	Dynamic Fiber Optic Strain Gages	2,3,4
	Dynamic Foil Strain Gages	4
	Dynamic Vibrating Strain Gages	3,4
	Fiber Bragg Grating (FBG) Accelerometers	3,4
	FBG Pressure Sensors	3
	Fiber Bragg Grating Laser (FBGL) Vibration Sensors	3
	Girder Edge Displacement Gages	3
	Global Positioning System (GPS)	3,5
	Long Period Grating (LPG) Sensors	3
	Pi Phase Shifted Grating Sensors	3
	Roadway Weather Sensor System	
	Tuned Mass Damper (TMD) Displacement Gages	3
Scour	Acoustic Distance Meters	2
	Contact Sensors	5
	Fiber Optic Scour Gages	5
	FBGL Hydrophones	3

CHAPTER 6

CONCLUSIONS

FTA is not a replacement for current risk assessment methods but in combination with visual inspection and SHM sensors it can make an improvement in the bridge management process. The fault-tree model allows for internal components to be assessed prior to visual inspections, which can help inspectors focus on the components that have a high influence on bridge failure and eliminate invasive inspection techniques that may be unnecessary. The model also allows events leading to bridge failure to be identified and assessed individually and as a system of events, which allows the impact of individual events and their relationships on bridge failure to be analyzed. These aspects make the qualitative analysis component of FTA a great tool for determining the initiating bridge failure events.

The quantitative analysis component of FTA can provide more useful information for bridge management, but numerous difficulties can arise. Often there is a lack of numerical data available on a basic event's contribution to bridge failure. In the James B. Edwards Bridge case study (Chapter 5), this issue was overcome by creating an undeveloped event at a high level with available data and eliminating the initiating events that had a lack of numerical data. The problem with this method is the initiating events that are the leading causes of the undeveloped event failure are unknown. Lab tests, finite element analysis (FEA) models, and field tests/observations over multiple years could provide more probabilistic data allowing all initiating events to remain in the fault-

tree for quantitative analysis; however, it is likely there will still be some events that have little numerical data available. For those events, expert opinion, sensitivity analysis, and probabilistic ranges can provide information accurate enough for use in countermeasure assessment and application. This was shown through the case study on the James B. Edwards Bridge.

For the James B. Edwards Bridge, the five most critical events that lead to bridge were found to be floods, scour, overloading, post-tensioning tendon corrosion and earthquakes. These critical events should be focused on by bridge management for the James B. Edwards Bridge, as well as other similar segmental concrete box girder bridges. Possible countermeasures were found for all of the critical events.

Since FTA probabilistic and validation data are sometimes difficult to find, the accuracy of the FTA results cannot be quantified with certainty. While FTA could be used as a tool for prediction of the age at which bridge failure will occur, more reliable probabilistic data would help the success of FTA as a bridge risk assessment tool.

In the future, FTA could be combined with NBI ratings, which are subjective, to quantify the risk of failure of each component. Since not all bridge types have the same risk of failure, FTA would have to be performed for each different bridge type. Then, the failure probabilities over a 50 year lifespan would be mapped to the median NBI rating estimate over the same 50 year lifespan. An example of this mapping procedure is briefly discussed in Appendix D.

The methods presented in this thesis are for assessment of an individual bridge. In order for bridges to be assessed as part of the transportation network, the consequence

of failure should also be analyzed. The addition of consequence would allow infrastructure managers to distribute their funds and time more effectively. Once the bridges with the highest risk have been identified within the network, FTA can be applied to the individual bridges as described in Chapter 3 to determine proper countermeasures.

APPENDIX A

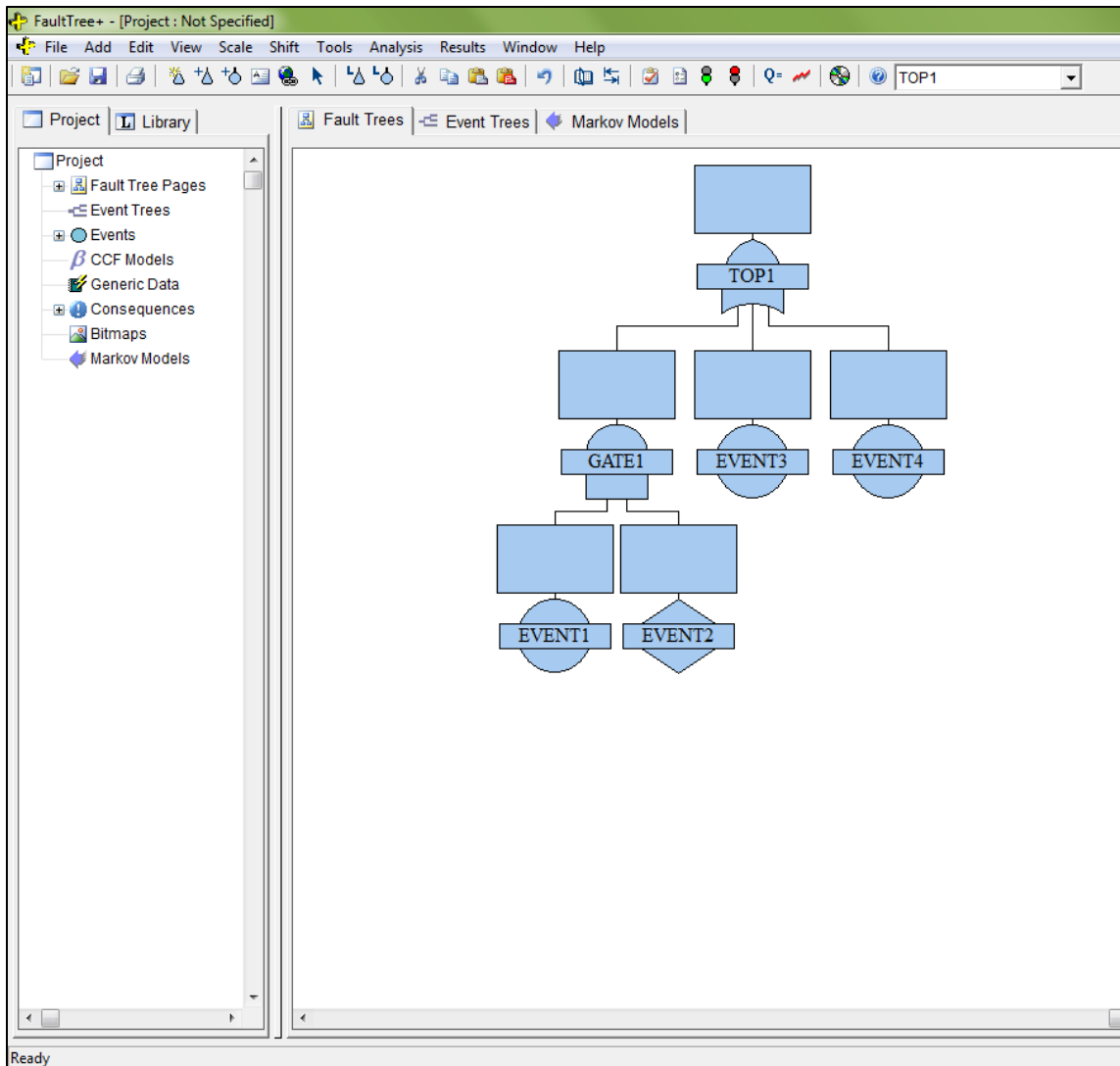


Figure A-1. Isograph FaultTree+ Interface

APPENDIX B

Complete list of the minimal cut sets for adjacent box girder bridge fault-tree:

- High Traffic Load
- Over Weight Trucks
- Fire
- Marine Collision with Beam
- Roadway Collision with Beam
- Train Collision with Beam
- Construction Error with Beam
- Deicing Salts \cap Water \cap Insufficient Water Barrier \cap Insufficient Grout
- Deicing Salts \cap Water \cap Insufficient Water Barrier \cap Dry Joint Construction
- Deicing salts \cap Water \cap Insufficient Water Barrier \cap Water Absorbent Material
- Seawater \cap Insufficient Water Barrier \cap Insufficient Grout
- Seawater \cap Insufficient Water Barrier \cap Dry Joint Construction
- Seawater \cap Insufficient Water Barrier \cap Water Absorbent Material
- Deicing salts \cap Water \cap Concrete Overstress
- Seawater \cap Concrete Overstress
- Deicing salts \cap Water \cap Insufficient Drain Size \cap Degradable Void Form \cap Open Void Form \cap Unsealed Vent Holes
- Seawater \cap Insufficient Drain Size \cap Degradable Void Form \cap Open Void Form \cap Unsealed Vent Holes
- Earthquake
- Storm Surge

- Flood
- Scour
- Marine Collision with Abutment or Pier
- Roadway Collision with Abutment or Pier
- Train Collision with Abutment or Pier
- Construction Error with Abutment or Pier
- Deicing salts \cap Water \cap Concrete Overstress
- Seawater \cap Concrete Overstress

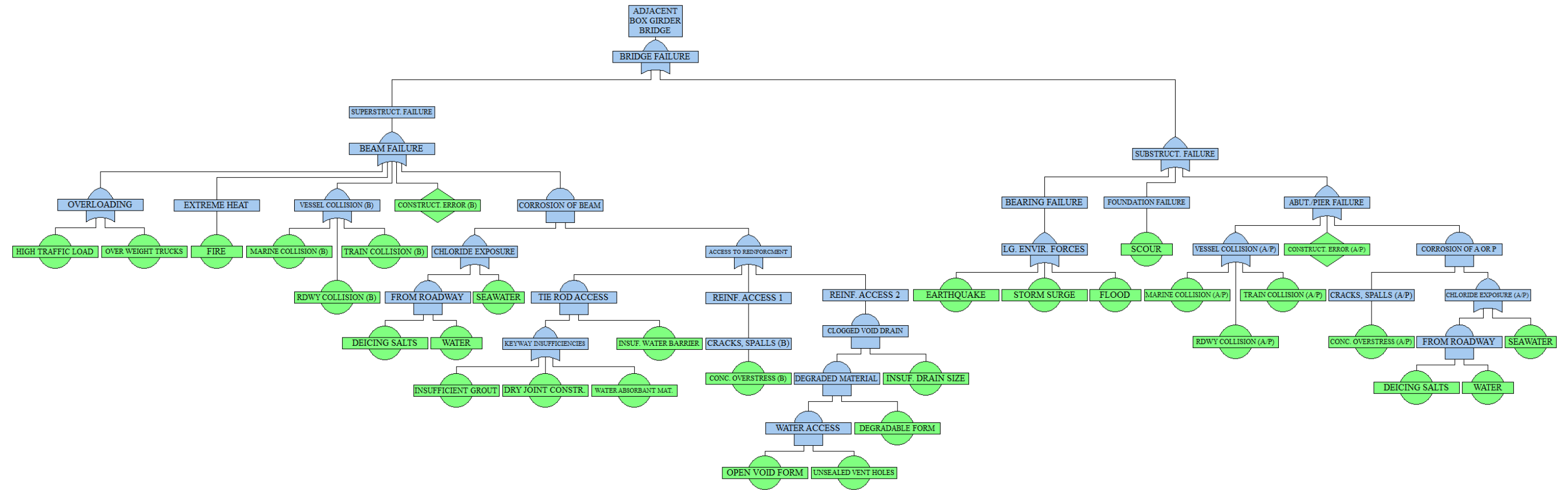


Figure B-1. Fault-Tree for Adjacent Box Girder Bridges

APPENDIX C



Figure C-1. Roadway beneath James B. Edwards Bridge



Figure C-2. James B. Edwards Bridge over Wando River



Figure C-3. View Inside James B. Edwards Bridge

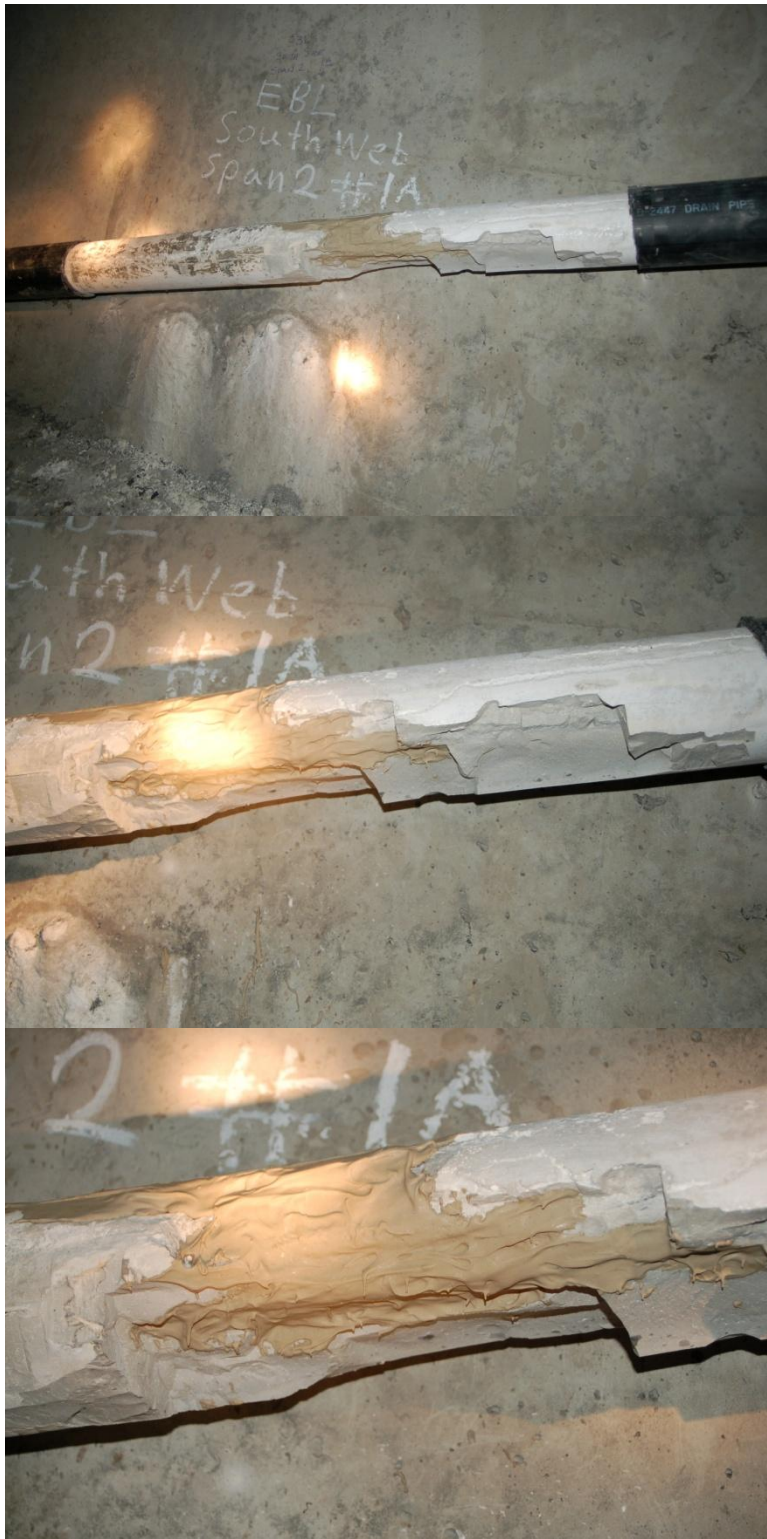


Figure C-4. James B. Edwards Bridge: Grout Voids and Tendon Exposure in Ducts



Figure C-5. James B. Edwards Bridge: Efflorescence from Leaky Joints



Figure C-6. James B. Edwards Bridge: Leaky Joint with Exposed Rebar



Figure C-7. James B. Edwards Bridge: Large Spall in Segment Roof near Joint



Figure C-8. James B. Edwards Bridge Bearing

List of minimal cut sets for James B. Edwards Bridge fault-tree:

- Overloading
- Fire
- Marine Collision with Beam
- Roadway Collision with Beam
- Construction Error with Beam
- Concrete-Corrosion of Beam
- Post-tensioning (PT) Tendon Corrosion
- Earthquake
- Storm Surge
- Flood
- Scour
- Marine Collision with Abutment or Pier
- Roadway Collision with Abutment or Pier
- Construction Error with Abutment or Pier
- Concrete-Corrosion of Abutment or Pier

Table C-1. Data Used for Calculation of Probabilities

Reference	Period	Period Range (N)	Avg. No. of Bridges	Failure Mode	No. of Failures	$P_{f,N}$
Harik	1951-1988	37	587717	Scour	6	1.02e-05
				Flood	8	1.36e-05
				Roadway Collision	19	3.23e-05
				Marine Collision	18	3.06e-05
				Overload	22	3.74e-05
				Fire	4	6.81e-06
				Sharma	1800-2009	209
Flood	695	1.16e-03				
Roadway Collision	86	1.43e-04				
Marine Collision	50	8.33e-05				
Overload	224	3.73e-04				
Fire	50	8.33e-05				
Construction Error	18	3.00e-05				
Earthquake	20	3.33e-05				
Storm Surge	16	2.67e-05				
Concrete-Corrosion & Conc. Deterioration	8	1.33e-05				
Wardhana	1989-2000	11	592966	Scour	78	1.32e-04
				Flood	165	2.78e-04
				Roadway Collision	14	2.36e-05
				Marine Collision	10	1.69e-05
				Overload	44	7.42e-05
				Fire	16	2.70e-05
				Construction Error	13	2.19e-05
				Earthquake	17	2.87e-05
				Storm Surge	2	3.37e-06
				Concrete-Corrosion & Conc. Deterioration	1	1.69e-06
Woodward				PT Tendon Corrosion		2.40e-06

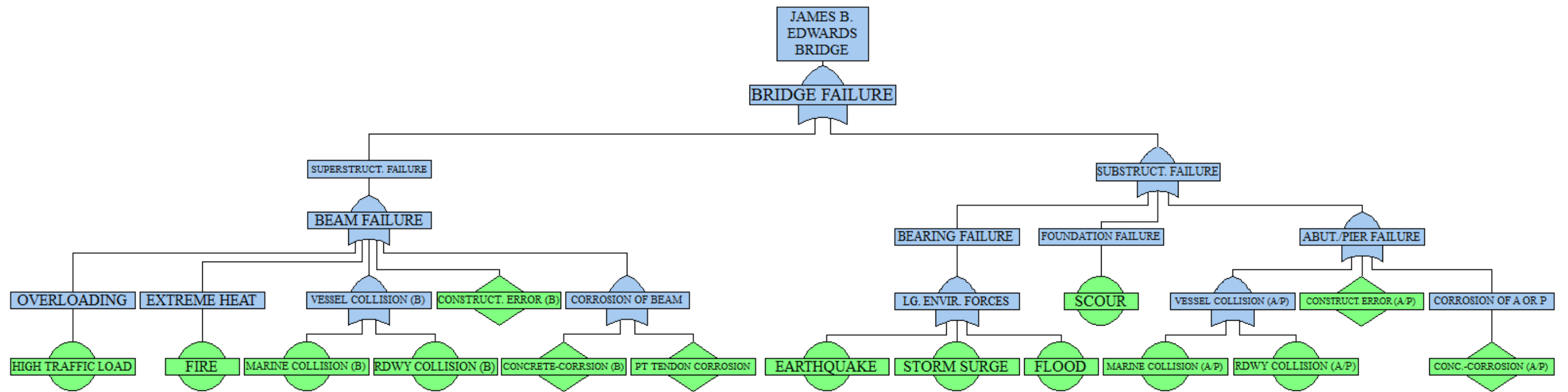


Figure C-9. James B. Edwards Bridge Fault-Tree

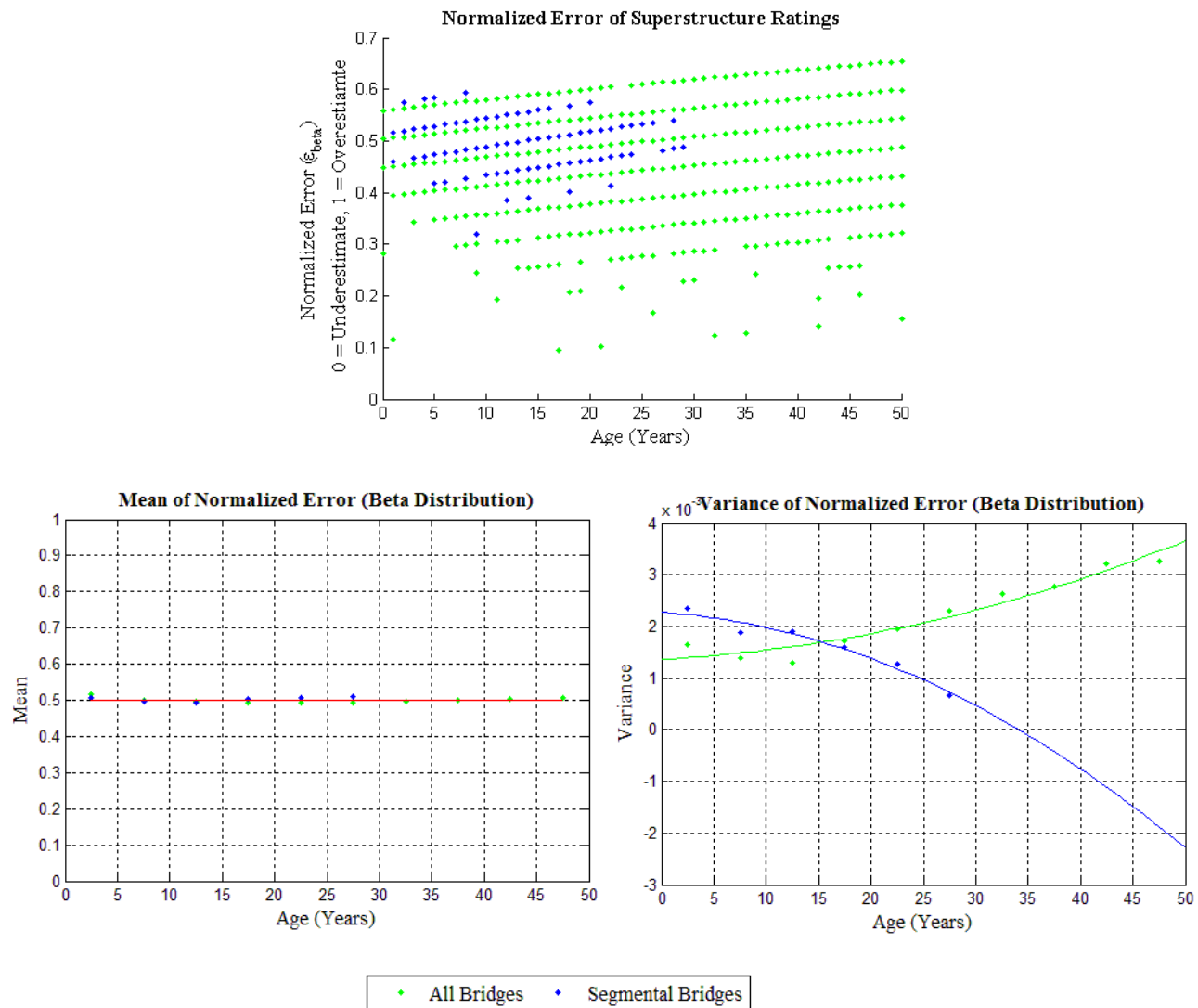


Figure C-10. NBI Superstructure Rating Error Comparison (a) Normalized Error (b) Mean (c) Variance

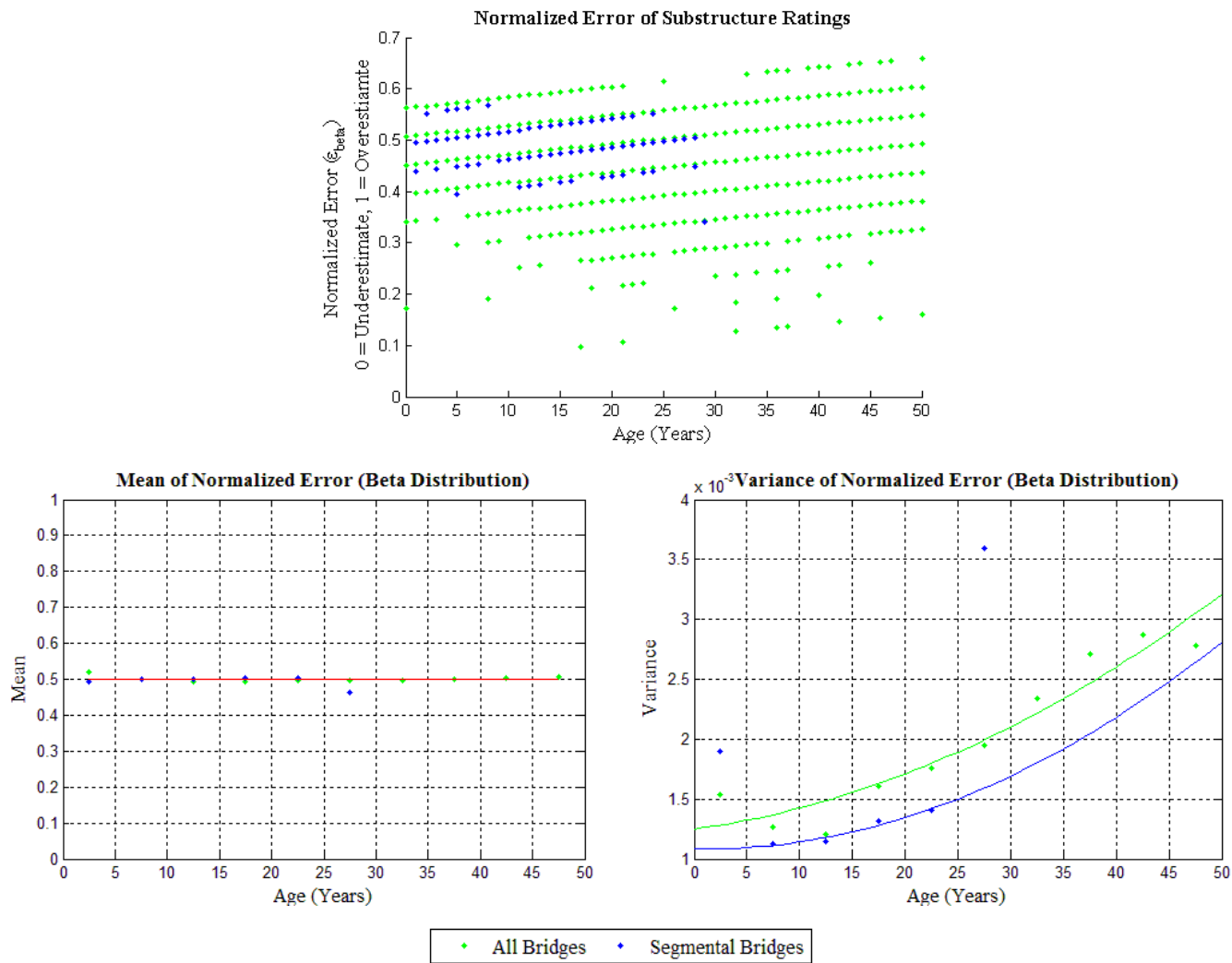


Figure C-11. NBI Substructure Rating Error Comparison (a) Normalized Error (b) Mean (c) Variance

Table C-2. Minimal Cut Set Ranking Based on Probability of Occurrence

Minimal Cut Set	Probability of Occurrence at Age 50
1 Flood	5.20e-04
2 Scour	2.30e-04
3 Overload	1.59e-04
4 PT Tendon Corrosion	1.20e-04
5 Earthquake	6.91e-05
6 Fire	3.90e-05
7 Construction Error (AP)	2.56e-05
- Construction Error (B)	2.56e-05
9 Storm Surge	1.09e-05
10 Concrete-Corrosion (AP)	5.43e-06
- Concrete-Corrosion (B)	5.43e-06
12 Roadway Collision (B)	2.61e-07
13 Roadway Collision (AP)	1.74e-07
14 Marine Collision (AP)	1.63e-07
15 Marine Collision (B)	5.43e-08

Table C-3. Examples of SHM Sensors for Applicable Minimal Cut Sets		
Minimal Cut Set	SHM Sensors	Ref*
Overloading	Weight-In Motion (WIM) Sensors	1,5
Fire	Fiber Bragg Grating (FGB) Temperature Gages	3,4
	Fiber Bragg Grating Laser (FBGL) Temperature Gages	3
	Stimulated Brillouin Scattering (SBS) Distributed Fibers	3
	Thermistors	4
	Thermometers	3
Concrete-Corrosion	Chirp Grating Sensors	3
	Dynamic Fiber Optic Strain Gages	2,3,4
	Dynamic Foil Strain Gages	4
	Dynamic Vibrating Strain Gages	3,4
	Fabry-Perot Interferometric Fiber Optic Sensors	4
	FBG Strain Gages	3,4
	FBGL Strain Gages	3
	Fiber Optic Michelson Interferometers	3
	SBS Distributed Fibers	3
	Chloride Sensors	5
	LPG Chemical Sensors	3
PT Tendon Corrosion	Chirp Grating Sensors	3
	Dynamic Fiber Optic Strain Gages	2,3,4
	Dynamic Foil Strain Gages	4
	Dynamic Vibrating Strain Gages	3,4
	Fabry-Perot Interferometric Fiber Optic Sensors	4
	FBG Strain Gages	3,4
	FBGL Strain Gages	3
	Fiber Optic Michelson Interferometers	3
	SBS Distributed Fibers	3
	Chloride Sensors	5
	LPG Chemical Sensors	3
Earthquake	Accelerometers	2,3,5
	Velocity Transducers	2
	Dynamic Fiber Optic Strain Gages	2,3,4
	Dynamic Foil Strain Gages	4
	Dynamic Vibrating Strain Gages	3,4
	FBG Accelerometers	3,4
	FBG Pressure Sensors	3
	FBGL Vibration Sensors	3
	Girder Edge Displacement Gages	3
	GPS	3,5
	LPG Sensors	3
	Pi Phase Shifted Grating Sensors	3
Seismometers	3	

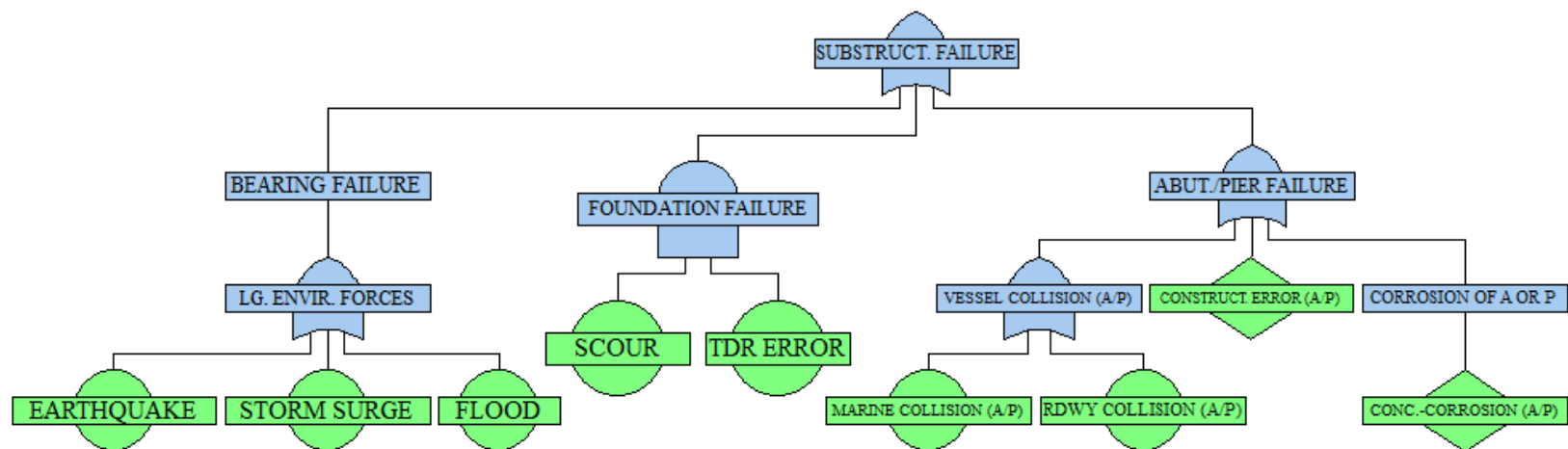


Figure C-12. Example Application of Countermeasure to James B. Edwards Bridge

APPENDIX D

MAPPING PROBABILITY OF FAILURE TO NBI RATINGS

Currently, the NBI ratings used by inspectors do not provide an insight on the likelihood of bridge failure. The mapping procedure described here combines NBI data and failure probabilities from FTA to develop failure probability estimates for each NBI rating. Since the substructure and superstructure are the main subsystems of a bridge, failure probabilities will only be applied to those subsystems. Even though the same NBI rating scale and descriptors are used for both subsystems, their corresponding probabilities of failure will not be the same. The probability of failure for each NBI rating will also vary by bridge type; therefore, the mapping procedure should be done for each bridge type listed in the NBI.

Development of Median NBI Rating Estimate

First, gather NBI superstructure and substructure rating data for similar bridge types from multiple states over several years. The data used could be from locations all over the U.S. or from states with similar environments. For this example, the substructure ratings for segmental box girder bridges from FL, NC, SC and VA for years 1994, 1998, 2002, 2006 and 2010 are considered. Once the data is gathered, create a scatter plot of the ratings over time as shown in Figure D-1. Then calculate the median estimate of the NBI ratings, \hat{R}_{NBI} , as a function of bridge age using an exponential decay function:

$$\hat{R}_{NBI} = c_1 \exp(-c_2 t) \quad (D-1)$$

where t is the bridge age (year) and c_1 and c_2 are regression parameters, which are determined using least-square fitting. An exponential decay function was chosen because it does not output a rating below the NBI scale, which ranges from 0 to 9. When data appears to have a more linear trend as in Figure D-1, a linear function can also be used but conditional bounds need to be applied.

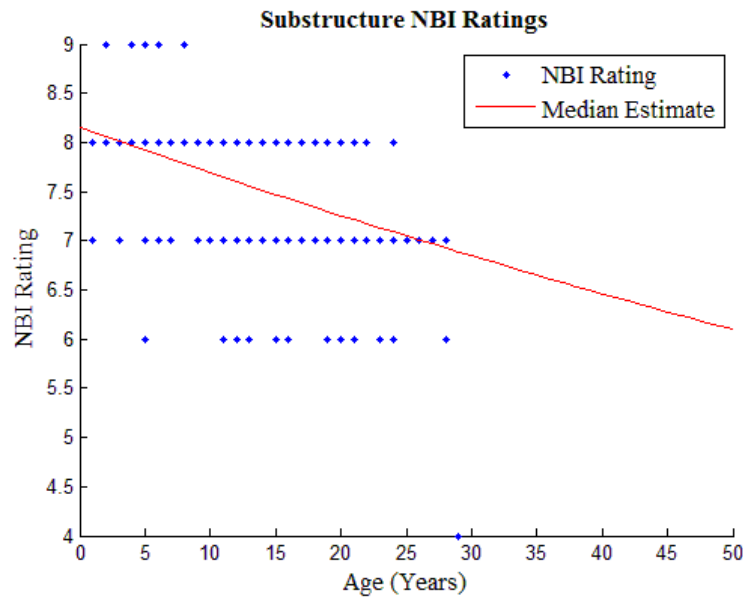


Figure D-1. Median Estimate of NBI Ratings versus Bridge Age

To assess the fitting of the median rating estimate, \hat{R}_{NBI} , in relation to the actual NBI rating, R_{NBI} , a normalized error term is defined:

$$\varepsilon = \frac{R_{NBI} - \hat{R}_{NBI}}{18} + 0.5 \quad (D-2)$$

where a normalized error value of 0.5 is defined as no error, 0 as an underestimate, and 1 as an overestimate. Then, fit the normalized error to Beta distribution, a continuous

probability distribution that defines a variable on the interval between 0 and 1. The cumulative distribution function (CDF) for the Beta distribution is:

$$F(\varepsilon|a,b)=\frac{1}{\beta(a_B,\beta_B)} \int_0^\varepsilon y^{a-1} (1-y)^{b-1} dy \quad (D-3)$$

where α_B and β_B are the Beta distribution parameters: $\alpha_B=\bar{\varepsilon}(\bar{\varepsilon}(1-\bar{\varepsilon})/v-1)$ and $\beta_B=(1-\bar{\varepsilon})(\bar{\varepsilon}(1-\bar{\varepsilon})/v-1)$, $\bar{\varepsilon}$ = mean, v = variance, and $\beta(\cdot)$ is the Beta function. For the Beta distribution, it is recommended that the NBI ratings be divided into multiple bins of equal age interval, preferably five-year intervals. Once each bin has been fitted to Beta distribution, the mean and variance of the normalized error for each bin can be computed using Equation D-2. Figures D-2 and D-3 show the mean and variance of the normalized error for the NBI substructure ratings from Figure D-1.

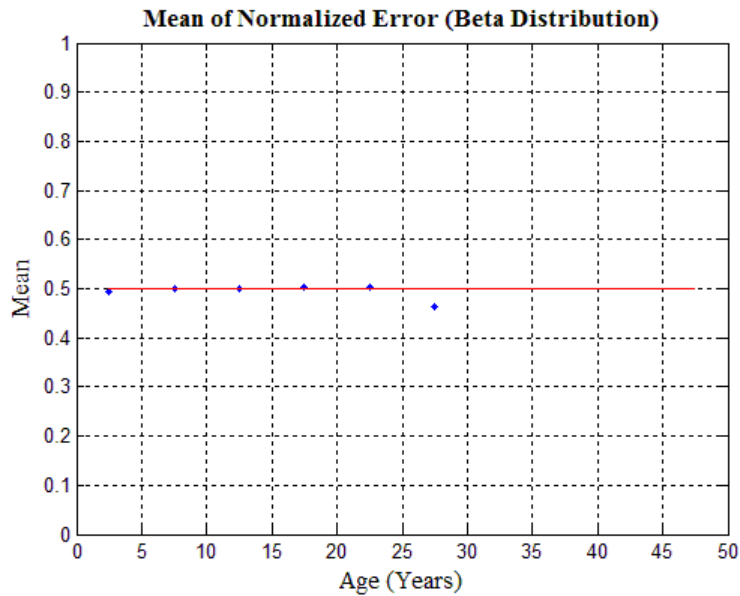


Figure D-2. Mean of Normalized Error versus Bridge Age

Figure D-2 shows the mean of the normalized error for all of the age bins are approximately equal to 0.5; therefore, for analysis purposes, the mean of the normalized error can be kept constant at 0.5. The assumption of constant mean value is justifiable since the normalized errors are randomly distributed around 0.5 and do not show any increasing or decreasing trend with age.

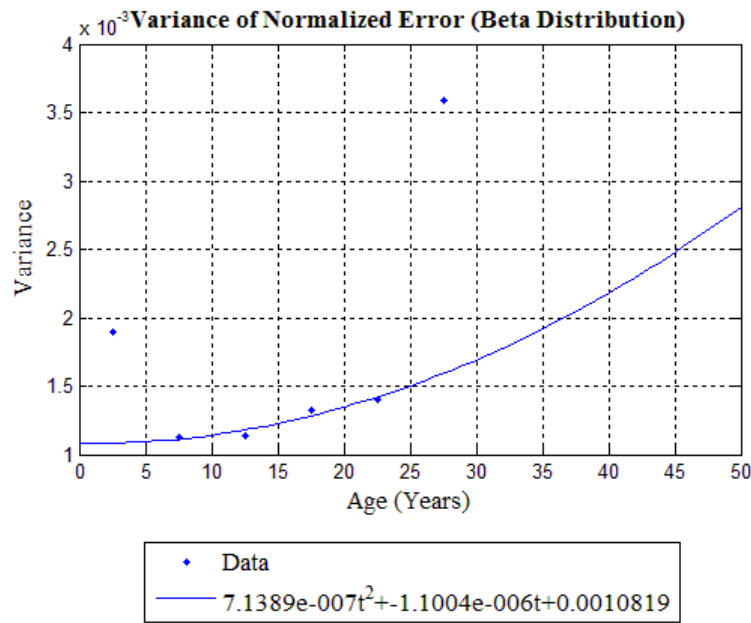


Figure D-3. Variance of Normalized Error versus Bridge Age

The overall variance in Figure D-3 shows an increasing trend with age. The increasing trend is due to the larger fluctuations in ratings that occur with age. To capture this trend, the variance values as a function of age are fitted to a second order polynomial equation:

$$v = a_2t^2 + a_1t + a_0 \tag{D-4}$$

where coefficients a_0 , a_1 and a_2 are determined using a least-square regression technique. It should be noted that bins from years 0 to 5 and 25 to 30 were not included in the fitting. Age bin 0 to 5 was excluded to show a continually increasing trend and bin 25 to 30 was excluded due to an outlier in the data set.

The mean (i.e. 0.5) and the variance function can be used to estimate the Beta distribution parameters (α_B and β_B) of the NBI ratings for each year. The new Beta distribution and calculated median estimate of the NBI ratings (Equation D-1) are then used for the procedure of mapping failure probability to the NBI ratings.

Calculation of Failure Probability

The methodology described in Chapter 3 can be used to calculate the failure probability of the subsystem (i.e. substructure, superstructure), which will be mapped to the NBI ratings. The failure probability of the substructure used for this example is shown in Figure D-4.

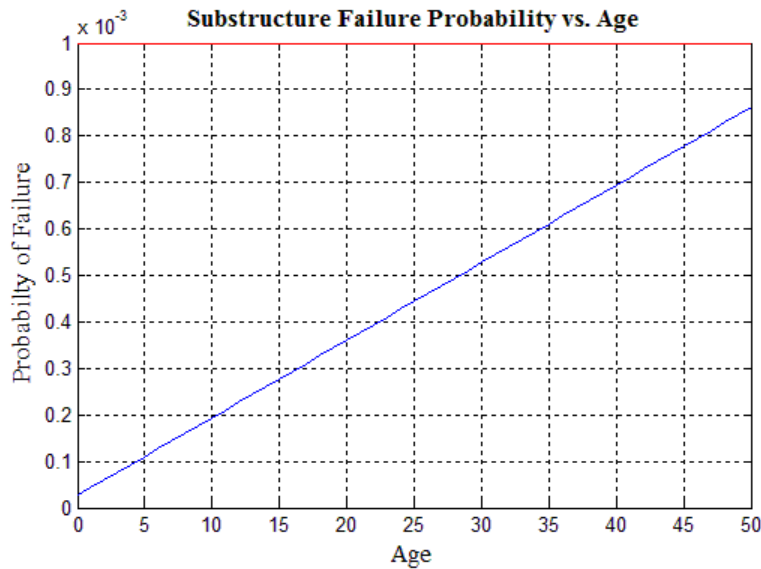


Figure D-4. Substructure Failure Probability versus Bridge Age

Mapping Procedure

The failure probability range will be assigned to each subsystem NBI rating. The range will be given from the 25th percentile to the 75th percentile. The first step is to find the year at which each NBI rating (i.e. 9, 8, 7, 6, etc.) occurs on the median estimate curve. Then, find the normalized error at the lower and upper bounds for those years. This can be calculated by taking the inverse of the cumulative Beta distribution function for a given year. Then, use the NBI rating (median estimate) and normalized error to calculate the lower/upper bound NBI rating using Equation D-2. Find the lower/upper bound rating on the median estimate curve. At the year the lower/upper rating occurs on the median estimate curve, find the corresponding failure probability using the FTA results. The results for the segmental concrete box girder bridge substructure example are shown in Table D-1.

The same procedure can be used for the superstructure. Once an NBI rating has been assigned to a substructure and superstructure of a bridge, their defined failure probabilities can be used to calculate the probability of bridge failure using Boolean algebra (same principles as FTA): (substructure failure) \cup (superstructure failure).

Table D-1. Example Results: Substructure NBI Ratings and Corresponding Failure Probabilities

Rating	Description	Failure Probability	Reliability
9	<u>Excellent</u>	< 2.63e-05	> 4.0
8	<u>Very good</u> : no problems	2.63e-05 – 2.24e-04	3.5 – 4.0
7	<u>Good</u> : minor problems	2.71e-04 – 6.64e-04	3.2 – 3.5
6	<u>Satisfactory</u> : some minor deterioration of structural elements	6.06e-04 – 1.25e-03	3.0 – 3.2
5	<u>Fair</u> : primary structural elements are sound but may have minor section loss, cracking, spalling or scour	9.27e-04 – 2.04e-03	2.9 – 3.1
4	<u>Poor</u> : advanced section loss, deterioration, spalling or scour	> 1.00e-03	< 3.1
3	<u>Serious</u> : loss of section, deterioration, spalling or scour have seriously affected primary structural components; local failures are possible; fatigue cracks in steel or shear cracks in concrete	> 1.00e-03	< 3.1
2	<u>Critical</u> : advanced deterioration of primary structural elements; fatigue crack in steel or shear cracks in concrete; scour may have removed substructure support; may be necessary to close the bridge until corrective action is taken	> 1.00e-03	< 3.1
1	<u>Imminent failure</u> : major deterioration or section loss present in critical structural components; obvious vertical or horizontal movement affecting structure stability; bridge closed to traffic but corrective action	> 1.00e-03	< 3.1
0	<u>Failure</u> : beyond corrective action; out of service	> 1.00e-03	< 3.1

REFERENCES

- Ansari, F (2009). "Structural Health Monitoring with Fiber Optic Sensors", *Frontiers of Mechanical Engineering in China*, 4(2), 103-110.
- Atamturktur, S (2011). Assistant Professor, "Structural Health Monitoring Tools for Bridges", Personal Communication, 2011 January 13
- de Brito, J., Branco, F. A., Thoft-Christensen, P., and Sorensen, J. D. (1997). "An expert system for concrete bridge management." *Engineering Structures*, 19(7), 519-526.
- Cambridge Systematics, Inc. (2005). "Pontis Modeling Approach Overview Presentation." FHWA, <<http://classic-web.archive.org/web/20071029003533/www.fhwa.dot.gov/infrastructure/asstmgmt/pontismodel.htm>> (May. 4, 2011).
- Chang, C. and Mehta, R. (2010). "Fiber Optic Sensors for Transportation Infrastructural Health Monitoring", *American Journal of Engineering & Applied Science*, 3(1), 214-221.
- Corven, J., and Moreton, A. (2004). *Post-Tensioning Tendon Installation and Grouting Manual*. Manual, U.S. DOT FHWA.
- Doebling, S. W., Farrar, C. R., Prime, M. B., and Shevitz, D. W. (1996). *Damage identification and health monitoring of structural and mechanical systems from changes in their vibration characteristics: A literature review*.
- Ericson, C. A., II. (1999). "Fault Tree Analysis - A History." *System Safety at the Dawn of a New Millennium*, System Safety Society, Orlando, FL.
- Farrar, C. R., and Worden, K. (2007). "An introduction to structural health monitoring." *Philosophical Transactions of the Royal Society A: Mathematical, Physical and Engineering Sciences*, 365(1851), 303-315.
- FHWA (1995). *Recording and Coding Guide for the Structure Inventory and Appraisal of the Nation's Bridges*. Report No. FHWA-PD-96-001. FHWA, U.S. Department of Transportation.
- FHWA (2011). "NBI ASCII Files." FHWA, U.S. Department of Transportation. <<http://www.fhwa.dot.gov/bridge/nbi/ascii.cfm>> (July 2011)

- Floyd, L. (2010). "SCDOT Bridge Maintenance Engineer Interview, 17 November 2010."
- Gutkowski, R. M., and Arenella, N. D. (1998). "Investigation of Pontis - A Bridge Management Software."
- Haasl, D. F., Norman, R. H., Vesely, W. E. and Goldberg, F. F. (1981). "Fault Tree Handbook." U.S. Nuclear Regulatory Commission, Report No. NUREG-0492, Washington, D.C.
- Harik, I. E., Shaaban, A. M., Gesund, H., Valli, G. Y. S., and Wang, S. T. (1990). "United States Bridge Failures, 1951-1988." *Journal of Performance of Constructed Facilities*, Vol. 4, No. 4, pp. 272-381.
- Harries, K. A. (2009). "Structural Testing of Prestressed Concrete Girders from the Lake View Drive Bridge." *Journal of Bridge Engineering*, 14(2), 78.
- Huang, Y.-H. (2010). "Artificial Neural Network Model of Bridge Deterioration." *Journal of Performance of Constructed Facilities*, 24(6), 597.
- Isograph (2008). *FaultTree+*, Version 11.2.4, Irvine, CA.
- Johnson, P. A. (1999). "Fault Tree Analysis of Bridge Failure due to Scour and Channel Instability." *Journal of Infrastructure Systems*, 5(1), 35.
- Karami Mohammadi, R. and H. Lahijanani (2010). "Developoing the Fragility Curves of Bridges Before and After Retrofitting by FRP." *Proceeding, 3rd fib International Congress*, Washington, D.C.
- LeBeau, K. H., and Wadia-Fascetti, S. J. (2007). "Fault Tree Analysis of Schoharie Creek Bridge Collapse." *Journal of Performance of Constructed Facilities*, 21(4), 320.
- MDOT. (2005). "Box-Beam Concerns Found under the Bridge: Expanding Inspector Handbook Promises Timely Bridge Care." *Construction and Technology Research Record*.
- Mufti, A. (2001). *Guidelines for Structural Health Monitoring*, ISIS Canada Corporation, Canada.
- Naito, C., Jones, L., and Hodgson, I. (2010a). "Development of Flexural Strength Rating Procedures for Adjacent Prestressed Concrete Box Girder Bridges." *Journal of Bridge Engineering*, 15(4), 408-418.

- Naito, C., Sause, R., Hodgson, I., Pessiki, S., and Macioce, T. (2010b). "Forensic Examination of a Noncomposite Adjacent Precast Prestressed Concrete Box Beam Bridge." *Journal of Bridge Engineering*, 15(4), 408.
- National Transportation Safety Board. (2008). Collapse of I-35W Highway Bridge, Minneapolis, Minnesota, August 1, 2007. Highway Accident Report, Wash.
- Pearson-Kirk, D. (2008). "The benefits of bridge condition monitoring." *Proceedings of the ICE - Bridge Engineering*, 161(3), 151-158.
- Russell, H. (2009). Adjacent precast concrete box beam bridges : connection details. Transportation Research Board, Washington D.C.
- Sharma, S., and Mohan, S. (2011). "Status of Bridge Failures in the United States (1800-2009)." TRB 90th Annual Meeting: Transportation, Livability, and Economic Development in a Changing World, Washington D.C.
- Sianipar, P. R. M., and Adams, T. M. (1997). "Fault-Tree Model of Bridge Element Deterioration Due to Interaction." *Journal of Infrastructure Systems*, 3(3), 103.
- Smith, D. W. (1976). "Bridge Failures." *ICE Proceedings*, 60(3), 367-382.
- Wardhana, K. and Hadipriono, F. C. (2003). "Analysis of Recent Bridge Failures in the United States." *Journal of Performance of Constructed Facilities*, 17(3), 144-150.
- Wenzel, H. (2009). *Health Monitoring of Bridges*, Wiley Online Library.
- Woodward, R. J. (1989). "Collapse of a Segmental Post-Tensioned Concrete Bridge." *National Research Record No. 1211*, (1211), 38-59.
- Woodward, R. (2001). "Durability of post-tensioned tendons on road bridges in the United Kingdom." *Durability of post-tensioning tendons, fib Technical Report, Bulletin 15*, Workshop 15-16 November, Ghent (Belgium).
- Worden, K., Farrar, C. R., Manson, G., and Park, G. (2007). "The fundamental axioms of structural health monitoring." *Proceedings of the Royal Society A: Mathematical, Physical and Engineering Sciences*, 463(2082), 1639-1664.
- Zhu, S., Levinson, D., Liu, H. X., and Harder, K. (2010). "The traffic and behavioral effects of the I-35W Mississippi River bridge collapse." *Transportation Research Part A: Policy and Practice*, 44(10), 771-784.